DESIGN AND CONSTRUCTION OF A HIGH-SPEED MATCHED INDEX OF REFRACTION FACILITY

A Thesis

by

JUAN R. REYES GONZALEZ

Submitted to the Office of Graduate and Professional Studies of
Texas A&M University
in partial fulfillment of the requirements for the degree of

MASTER OF SCIENCE

Chair of Committee, Mark L. Kimber
Committee Members, Karen Kirkland
Jorge Alvarado
Head of Department, Yassin Hassan

August 2018

Major Subject: Nuclear Engineering

ABSTRACT

The design and construction of a recirculating high speed matched index of refraction facility will aim to provide a deeper understanding of isothermal turbulent mixing at a fundamental level. The understanding of this fluid flow phenomena will allow a greater understanding of the thermal hydraulic challenges found in generation IV (Gen IV) reactors and fluid thermal systems. Particle image velocimetry combined with matching index will provide unobstructed data acquisition and increase optical access in the region of interest. Mineral oil is used, as the working fluid, in combination with two 24-inch long quartz plate to achieve index matching. The two quartz plates will be inserted in a test section which will form three channels. The test section was designed with the goal of achieving a slot channel Reynolds number of at least 10,000. A 5^{th} order polynomial contraction was also designed with the propose to generate a uniform velocity profile before the test section's inlet. In conjunction with the contraction, a flow conditioner was place three hydraulic diameters upstream of the contraction's inlet with the goal to reduce turbulence intensity in the flow. Two expansions were also designed in order to connect different pipe sizes and geometries in the pipe system while minimizing flow separation. The pressure drop of the system was theoretically analyzed and a 20 horsepower inline centrifugal pump was selected based on the results and it is expected to operate with an efficiency between 86% and 79%. Design and construction of the facility is completed along with filling the facility with mineral oil. Leaks in the system were

addressed and fixed in order to ensure a leak tight construction. After the building electrical accommodations are adjusted, experiments can be initiated.

DEDICATION

To my parents, who supported me through the many challenges I encountered and to my brother, who set the example of achieving success.

CONTRIBUTORS AND FUNDING SOURCES

Contributors

This work was supervised by a thesis committee consisting of Dr. Mark Kimber and Dr. Karen Kirkland of the Department of Nuclear Engineering and Dr. Jorge Alvarado of the Mechanical Engineering Department.

The construction of the experimental facility was possible with the help of Nicholas Knight of the Department of Nuclear Engineering, Paul Kristo of the Department of Mechanical Engineering, Corey Clifford of the Department of Nuclear, Engineering, Troy Stepan (Facilities Coordinator III) of the Nuclear Engineering Department, Dr. Hassan's lab group from the Department of Nuclear Engineering, and Dr. Shao's lab group from the Department of Nuclear Engineering.

Funding Sources

The research was performed using funding received from the DOE Office of Nuclear Energy's Nuclear Energy University Programs.

TABLE OF CONTENTS

Page

LIST OF FIGURES

Page

LIST OF TABLES

Page

1 INTRODUCTION AND PROJECT OVERVIEW

1.1 Introduction

The purpose of constructing this facility is to study isothermal turbulent mixing across complex geometries at its most fundamental level, and to provide high quality data for future efforts in modeling validation. Particle Image Velocimetry (PIV) combined with index matching will be used as the measurement means to minimize obstruction when gathering data. The flow will be traveling at high enough speeds such that a slot channel Reynolds number of at least 10,000 is achieved. The use of this facility will help obtain better insight into turbulent mixing. Understanding the physics involved will allow for improved designs in the thermal hydraulics of Generation IV (Gen IV) reactors and many other applications. Advancement in Gen IV reactors is of great importance because of the urgent necessity of other safe and reliable forms of energy production.

Gen IV reactors are the leading candidate for the next generation reactors due to the passive safety design requirements such as cooling via natural convection during a loss of flow scenario [2]. As part of the Gen IV reactors, sodium cool fast reactors (SCFR) and high temperature gas reactors (HTGR) are good candidates. Although they meet safety criteria in many ways, there are known thermal hydraulic challenges that need to be studied and addressed. The flow physics in the lower plenum of HTGR are similar to those found in the combination of an impinging jet and flow across a bank of cylinders. At the

outlet region, potential mixing of the flows at different temperatures can caused thermal fluctuations [3, 4]. This phenomenon is also known as thermal stripping and it is identified as one of the causes of thermal fatigue in nuclear power plants [5]. In the 1980's, rapid changes in coolant temperature were first observed in liquid cooled reactors. These changes in temperature occur in components near the cooling channels. The rapid temperature fluctuations cause expansions and contractions to the reactors materials which induce fatigue and cyclic creep damage [6]. Propagations of surface cracks was also observed on stainless caused by thermal shock (thermal striping) up to temperature of 650°C [7]. The leading cause for thermal striping is improper mixing of the fluid. Many studies have been conducted on a triple jet configuration with the central jet at a lower temperature from the two adjacent jets. For the isovelocity case, convective mixing was observed about the center cold jet. Convective mixing did occur, for the non-isovelocity case, but it yielded higher post-mixing temperature compared to the isovelocity case [8]. The conclusion of this study shows that careful attention should be given to the velocity and temperature of the cooling channels that will undergo mixing to achieve adequate cooling in nuclear reactors. A numerical investigation using large eddy simulation (LES) was conducted on parallel triple jets and it showed good agreement with the results found by Tokuriho and Kimura [8] and Cao et al. [9]. In the coolant channels of the HTGR, helium flows at a velocity of approximately 70m/s [10]. The high flow velocity into the lower plenum is a contributor to many heat transfer and safety issues. Another of the issues found in the study is hot spots due to the complex geometries found in the lower plenum which can results in inadequate cooling to occur in certain locations [11]. The lower

plenum of HTGRs needs to be studied carefully since different flow characteristic can be found depending on how close the region of interest is to the lower plenum's outlet. The magnitude of the effective crossflow will be higher near the outlet than further away. This behavior of the crossflow leads to behaviors dominated by the jet flow in certain regions which can required refined modeling in order to capture the physics of the hots spot formation [3, 4]. Similar to the HTGR, sodium cool fast reactors also experience thermal stripping. The phenomenon occurs in the above core plenum due to the mixing of the cooling channels and core breeder sub-assemblies [12]. In SCFR, loss of coolant incidents occurs due to high cycle thermal striping which results in thermal fatigue. Kimura et. al. conducted a triple jet experiment with a stainless steel plate parallel to the jets. The objective of the experiment was to quantify the characteristics of the fluctuations in the temperature from the fluid to the structure. The study concluded that that region of high thermal fluctuations became more localized as it approached the surface of the wall [13]. These same thermal hydraulic problems are not limited to nuclear reactors but are also found in mixing tees and elbows in pipe systems [14, 15]. The broader impact of research conducted with this design of a matched index of refraction facility is to not only to enhance performance and safety of these advanced reactors but other fluid and thermal systems as well since these metrics are affected both directly and indirectly by the turbulent flow conditions in the systems. The generation of high fidelity data also provides future modelers with trusted benchmark data to help validate their approach in capturing turbulence. It should be noted that although many of these examples cited above relate to temperature fluctuations, these are heavily influence by the average velocity field and the

spectrum of turbulent energy fluctuations. While other facilities focus on the non-isothermal aspects of turbulent mixing, this facility takes a step towards the fundamentals in that it will provide the detailed measurements needed to first assess the turbulence modeling capabilities.

1.2 Existing MIR Facilities and Water Tunnels

The design of this high Reynolds number matched index of refraction (MIR) facility was inspired by the design of existing recirculating flow facilities, including the Idaho National Laboratory (INL) MIR facility design and those from Ripken [16], Nedyalkov [17], and Daniel [18]. Studying these designs facilitated determination of the necessary components as well as the effect they have on the flow. In this section, a brief description of each of these facilities will be discussed.

Idaho National Laboratory MIR Facility

The purpose of this facility is to study of flow phenomenon that occurs in the lower plenum of a prismatic core Very High Temperature Reactor (VHTR) and generated high quality data for validation of computational fluid dynamic (CFD) codes. It consists of a primary loop that recirculates mineral oil at approximately 9510 gallons per minute (gpm) and achieves a maximum velocity of 5.6 ft/s at the test section's inlet. In addition to the primary loop, there are two auxiliary temperature control loops. The first auxiliary loop extracts approximately 80 gpm and runs parallel to the primary loop and recombines downstream of the axial pump. In order to maintain proper temperature control, the

auxiliary loop contains a glycol-cooled heat exchanger and a 10kW DC heater. The second auxiliary loop contains the same temperature control system but it is also used to provide fluid to the jet inlets found in the experimental model, as shown in Figure 1The test section is composed of three 2 ft × 2 ft cross sectional area and has a combined length of 8 ft. Inside of the test section, the experimental model can be found, which is composed

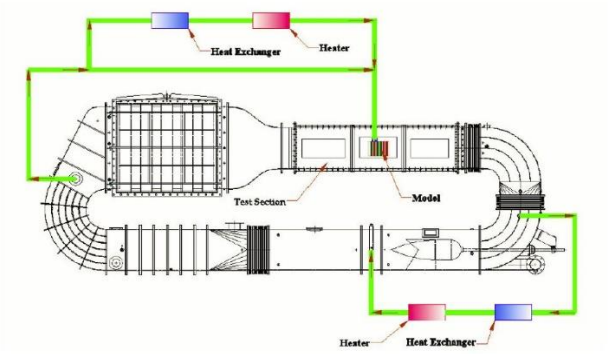

Figure 1 - INL Temperature Control System [19].

of a bank of cylinders made out of quartz which replicates a scaled lower plenum of the VHTR. As previously mentioned, the experimental model also contains jet inlets which are connected to a manifold that feeds from one of the auxiliary loops. The experimental model arrangement allows for cross flow from the primary loop and vertical flow from the jets which are similar conditions found in the lower plenum of a VHTR as shown in Figure 2 [19].

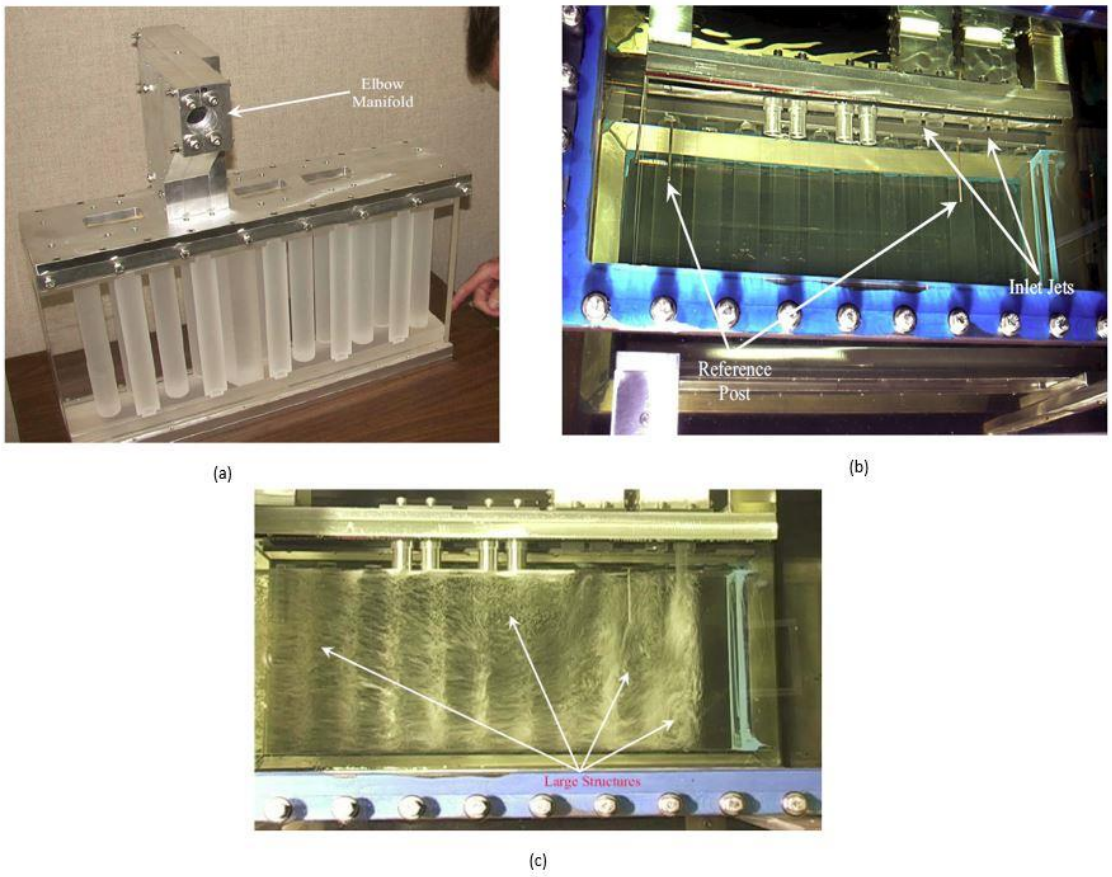

Figure 2 - (a). Experimental Model[19]. (b). Close up of MIR Test Section and Experimental Model [19]. (c). Flow Visualization of Four Jets [19].

Chalmers University of Technology High Speed Water Tunnel

This high speed water tunnel facility was designed with a focus on the flow's boundary layer growth and cavitation number inside a 6 in × 6 in test section. The flow is motivated by an axial pump which is capable of achieving velocities of approximately 6.56 ft/s to 39 ft/s inside of the test section. The flow's velocity was determined using: Particle Tracking Velocimetry (PTV), Laser Doppler Velocimetry (LDV), Particle Image Velocimetry (PIV), and Differential Pressure Measurements. The water tunnel consists of

26 major components as shown in Figure 3a. At location 0, the test section can be found which is connected to a square to rectangle transition/diffuser (1 and 2). Downstream of the diffuser, corner 1 can be found which consist of parts (3-5) where 4 is a turning vane, such as found at locations 8, 16, and 20. The first corner is followed by another diffuser (6) and the second corner (7, 8, 9). At the second corner is where the axial pump can be found which connects to the straight piping (10-14). Further downstream, corners 3 and corners 4 (15-21) are found. Lastly, a short straight pipe (22) connects to a honeycomb (23) and lastly to a modified straight pipe and 5th order polynomial contraction (25). The assembly of the water tunnel is shown in Figure 3b [17].

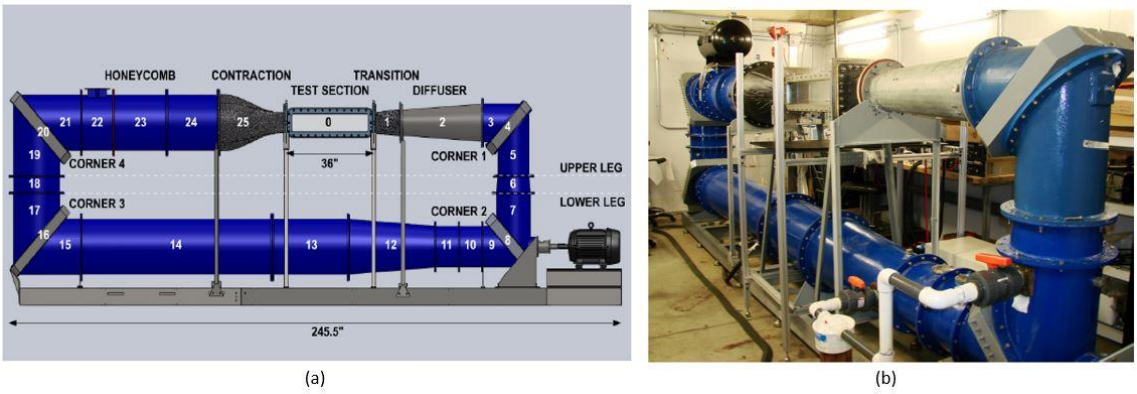

Figure 3 - Chalmers Water Tunnel Facility.

Oklahoma State University Water Tunnel

The primary purpose of this facility is to conduct drag reduction experiments for naval applications. The facility achieves a volumetric flow rate of 4500 gpm and reaches a momentum thickness-based Reynold number in excess of 10^4. The test section is made out of acrylic for optical access in order to use PIV as the primary high speed flow

visualization. Inside the 6 in × 6 in test section, flow speeds higher than 32.8 ft/s are possible. The system is pressurized to 40 psi to avoid sudden pressure drops and poor flow quality due to cavitation. The water tunnel is composed of 16 primary components as shown in Figure 4 [18].

Part Number	Description	Part Number	Description
1	Elbow 1	9	Down Leg Piping
2	Honeycomb (HC1)	10	Elbow 3
3	Settling Chamber and Honeycomb (HC2)	11	10" X 12" Rolled Cone
4	Contraction	12	Pump Inlet Piping
5	Test Section	13	Pump and Motor
6	Diffuser	14	10' X 20" Rolled Cone
7	Straight Pipe	15	Elbow 4
8	Elbow 2	16	Up Leg

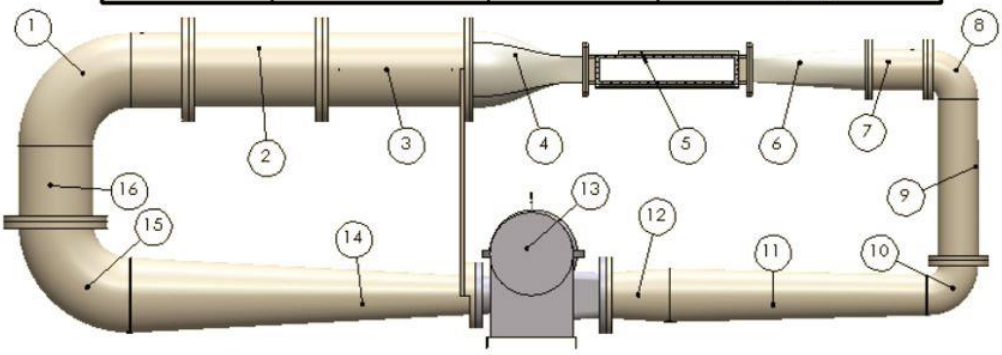

Figure 4 - Oklahoma State Water Tunnel.

1.3 Facility Components

In the following section, the facility components are briefly discussed. The goal of this section is to describe the purpose of these important components. A more detailed discussion of the design parameters of each component will be described in greater detail in chapters 2-4. The following descriptions will be used referring to Figure 5.

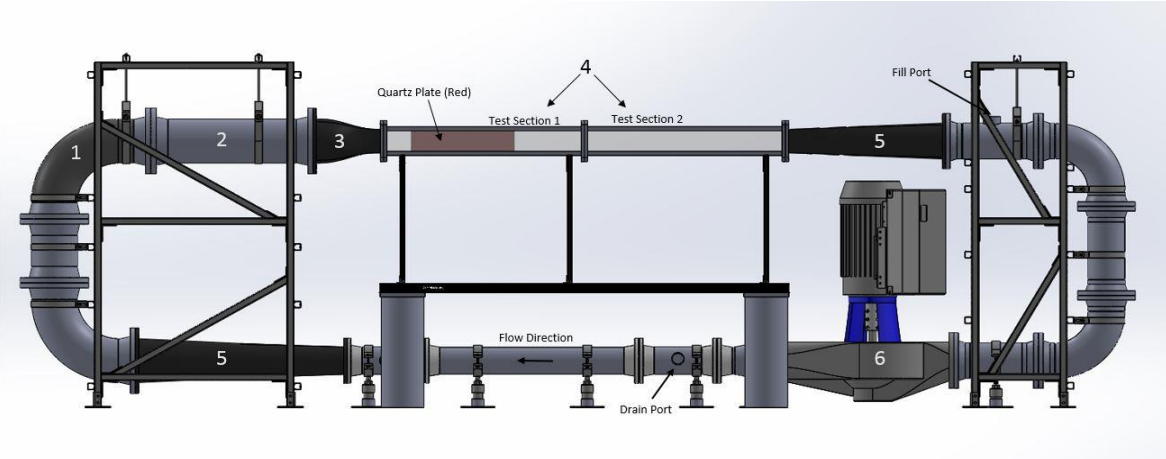

Figure 5 - Facility Overview.

1. Flow Conditioning Unit

A flow conditioning unit is usually used to eliminate or reduce turbulent intensity of a flow. This device removes swirls in the flow that impede an accurate measurement in the point of interest. The installation will improve the data acquisition's accuracy by producing a developed flow profile, therefore eliminating the flow disturbances caused by the loop's piping. For this facility, an elbow with fins on the inside is used as the flow conditioner.

2. Settling Chamber

The settling chamber works in conjunction with the flow conditioning unit. In order to obtain a fully developed profile, a straight pipe after the flow conditioner can be used. As recommended by the manufacturer, the settling chamber's length should be three hydraulic diameters. In this case, since the

pipe size at this point is 10 inch nominal, a 30-inch-long settling chamber was installed.

3. **Contraction**

The main propose of a contraction is to increase the flow's velocity and reduce turbulent intensity. In addition, the contraction is also used to generate a flat profile of the flow, which for this case it is desired in the entrance of the test section.

4. **Test Section**

The test section is where all of the data gathering will take place. It is the place where the physics of interest will be captured. Therefore, the test section was the first component designed to ensure the necessary flow properties such as Reynolds number is obtained. Design constraints for all other components are dictated by the test section dimensions.

5. **Diffuser**

The diffuser reduces the flow's velocity while increasing its pressure. There are two diffusers in the facility, the first one is directly downstream of the test section and the second one is found in the return leg of the loop.

6. **Pump**

   A pump is a device that provides motion to a fluid (liquid or gas) by compressing the fluid through a mechanical motion.

The pipe system is composed of stainless steel schedule 10 piping. The mentioned schedule was selected since it provides the necessary structural rigidity while reducing the system's weight as compared to the standard schedule 40. Stainless steel pipes were selected to prevent corrosion in the system. The experimental facility length of 21.7 ft and a maximum height from the ground of 8.2 ft as shown in Figure 6. The facility will be filled with approximately 120 gallons of Drakeol 5 light mineral oil.

Figure 6 - MIR Facility.

2 TEST SECTION

2.1 Technical Specifications & Manufacturing

The test section is composed of two similar assemblies that are connected together via a bolted connection. Both of the assemblies have internal dimensions of a 2 in by 5 in rectangular cross sectional area and each of them extend 47 in for a total length of 94in. The first assembly contains two 5 in x 0.25 in x 24 in quartz plates which will form three channels where the flow will be separated. The three channels are positioned 6 inches from the beginning of the test section and extend for 24in. After the flow travels 24in in the three channels, it will be recombined in the mixing channel. The three channels consist of two identical channels at the side (channel 1) and a narrower channel (channel 2) in the middle. The dimensions for the side channels are 5in tall and 0.563in wide, while the middle channel is 5in tall and 0.375in wide. These dimensions were chosen since it creates a good balance between pressure drop and flow velocity in order to achieve the desired flow conditions. The flow being driven through these channels will experience the same

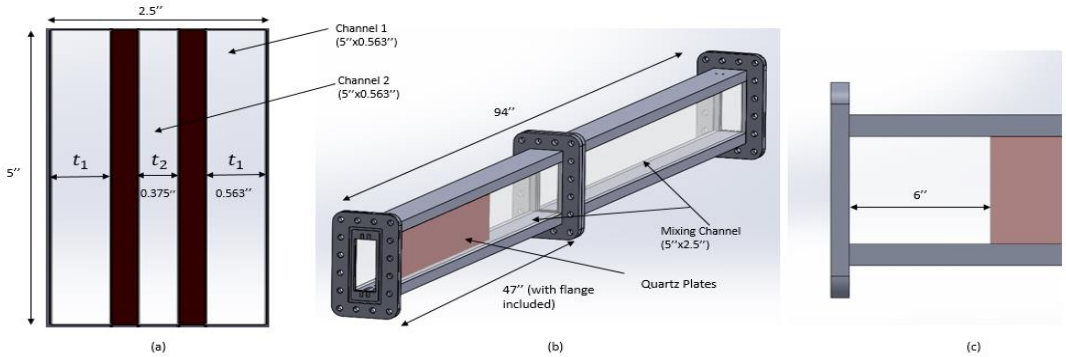

Figure 7 - (a) Test section inlet with quartz plates (red). (b) Test section assembly.(c) Side view of test section's inlet.

pressure drop across the 24 in length of the quartz plates. The dimensions of the channels are chosen based on the desire to achieve respectible velocity differences in the channels withouth incrurring a large pressure drop.

The test section is made from acrylic since it provides optical access and simplifies the machining process. Each of the two test section assemblies consists of 6 components: top/bottom window, left/right window, and front/back flanges. The dimensions of these windows and flanges are identical for both test section assemblies, with the exception of the top/bottom windows of the first test section. Here, there are accommodations made for the quartz plates. Specifically, there are two 24 in long grooves (see Figure 2(a)) machined in both the top and bottom windows, which allow the quartz plates to be slid in during assembly (see Figure 2(b)). The length of the groove is actually greater than the length of the quartz plates. This allows for a 6 in section of flow before the separation into the center and outer channels occurs. Allowing for 0.5 in for the flange on either side of the test

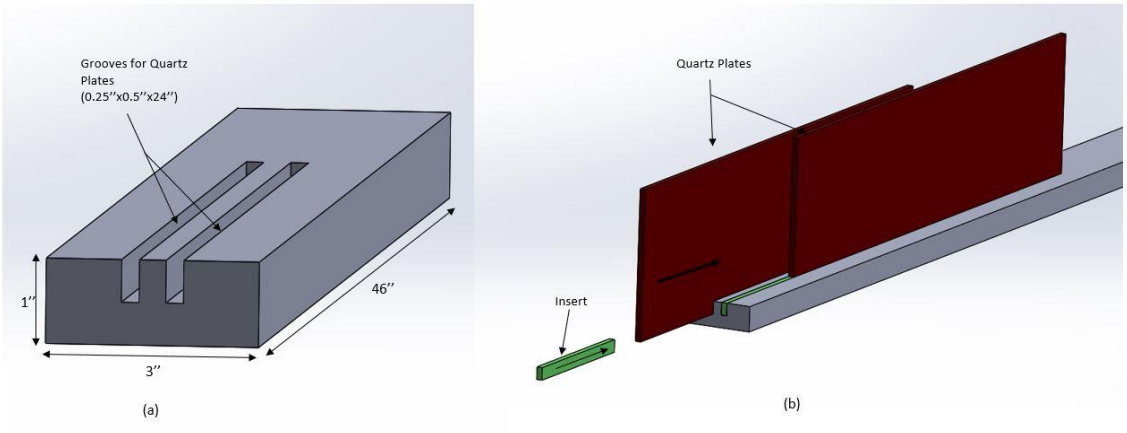

Figure 8 - (a) Top/Bottom Window with grooves. (b) Exploded View of Quartz Plates (red) and Inserts (green) in Top/Bottom Window.

section assemblies and making use of the fact that 1 in thick pieces of acrylic will be used for these top/bottom windows, their dimensions are 3 in x 46 in. As shown in Figure 8b, the quartz plates slide into the top/bottom window's grooves. The inserts (0.25 in x 0.5 in x 6 in) also slide in after the quartz plates and then are held in place by a small screw that attaches to the top and bottom windows from the outside of the test section. This allows the quartz plates to be removed from the test section while maintaining a flat and uniform surface inside the test section. The side windows are also made from acrylic but the thickness is reduced to 0.5 in since no actual machining is needed for these components. The height and length of these side pieces is 5 in and 46 in, respectively. A thickness of 0.5 in will also significantly decrease any refraction when PIV data is being collected due to reduction of material imperfections. The last components of the test section are the flanges. Three different designs of flanges were made: model A, B, and C. The model A flange was design in order to accommodate a gasket and quartz plates grooves, model B accommodates a gasket, while model C represents the mating gasket for model B, and therefore has a flat face at the connecting interface. Moreover, test section 1 uses a model A flange in the front and a model B flange in the back. Test section 2 uses a model C flange in the front and a model B flange in the back. This arrangement allows for a gasket to be placed at the interface of the contraction and test section 1, another one between test section 1 and 2, and a third gasket between test section 2 and short expansion that follows downstream. Figure 9 illustrates the different flange models. A detailed drawing of the flanges with all dimensions and corresponding tolerances are provided in Appendix A.

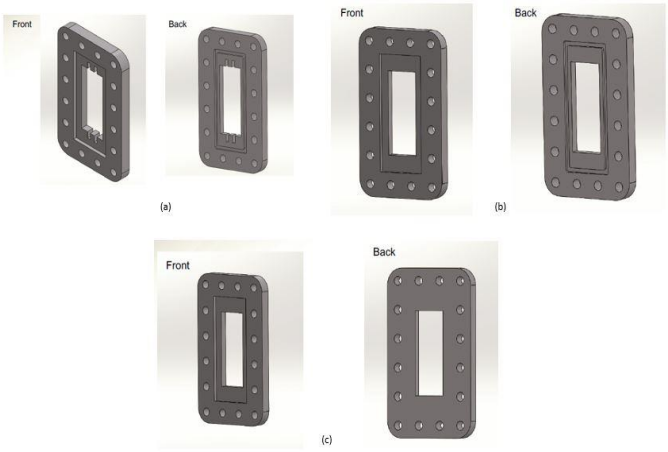

Figure 9 - (a) Model A Flange. (b). Model B Flange. (c). Model C Flange.

For a quick overview, the flanges have a height of 10 in, width of 6 in and a thickness of 0.75 in. The flange is connected via 1/2-13 TPI square bolts which are secured with the corresponding grade 5 hex nuts. Also, oversize washers (0.531 in ID, in OD) were used on both sides with the purpose to avoid or reduce indentations in the fiberglass (contraction and short expansion) and the acrylic. There are a total of sixteen 0.532" thru holes where the bolts are installed for a uniform connection across the mating faces and proper gasket connection.

The gaskets are made of Nitrile (NBR 60-A DURO), which was selected based on its good properties with sealing oil. The gasket has a thickness of 0.188" which is kept in place using the 0.163" deep grove machined in the gasket face. A 13.3% squeeze was achieved which was enough to ensure a leak tight seal. This metric can be calculated using Eq (2.1).

$$Squeeze\ \% = \frac{(w - g)}{w} \times 100 \tag{2.1}$$

2.2 Operating Condition

In order to ensure turbulent mixing occurs, a Reynolds number of at least 10,000 is desired in both the side channels (channel 1) and the middle channel (channel 2). Based on the pressure drop of the system the approximate minimum target flow rates are illustrated in Table 1. Moreover, it should be mentioned that the values shown below will be different from the actual operating conditions since the pump's performance curve along with the operating frequency will determine the actual flowrate. The expected real world flow rate is approximately 1200 gallons per minute (gpm) at the inlet, which is above the minimum requirements.

Table 1 - Minimum flow requirements.

Parameter	**Main Channel**	**Channel 1**	**Channel 2**
Volumetric Flow Rate (gpm)	806	321	164
Flow Velocity (m/s)	7.88	11.16	8.54
Reynolds Number	3.84×10^4	1.93×10^4	1.0×10^4

3 CONTRACTION AND EXPANSION

3.1 General Overview

The design parameters utilized for the contraction and expansions are discussed in this chapter. Parameters such as length, shape, inlet, and outlet dimensions will be reviewed. Manufacturing for these components was done by Diehl Aero-Nautical Co. and fiberglass was selected as the construction material. A 3/8-inch thickness was chosen based on simulation studies done by Daniel [18].

3.2 Contraction

A 5^{th} order polynomial profile was selected for the contraction shape. As demonstrated by Bell and Metha [20], this curve fit will reduce turbulence intensity and generate a flat velocity profile. As found by Ripken [16], a simple and powerful way to adjust a distorted velocity profile is modifying the area ratio of contraction (A_{ci}/A_{co}) which is the inlet area over the outlet area of the contraction. Furthermore, Ripken also stated that in general, water tunnel designs have an area ratio of contraction between 6 and 9. For the contraction design, a ratio of 7.9 using 10-inch nominal piping and contraction inlet diameter was achieved since it provided a good agreement with pump size requirements and economic constraints. The final parameter to fully define a contraction design is the length contraction ratio (L_c/D_{ci}). The definition of the mentioned parameter is the length of the contraction over the inlet diameter. The value for this ratio is based on CFD studies performed by Nedyalkov [17]. The mentioned study concluded that for a

length contraction ratio of 1.5 the velocity variation between the maximum velocity and the center-line velocity is slightly larger than 1%. Moreover, for a length contraction ratio of 1.6, the variation of the maximum velocity and the centerline velocity showed to be less than 1%. Although this ratio generates a flatter velocity profile, 1.5 was selected for the length of contraction ratio in the current design due to space constraints. Furthermore, it should be mentioned that the velocities used for the aforementioned CFD studies are very close to the design velocity of this facility. A 5^{th} order polynomial can be defined as shown in Eq. (3.1) and in Daniel and Nedyalkov. [17, 18].

$$Y_c = Y_{ci} - (Y_{ci} - Y_{co})\left[6\left(\frac{X_c}{L_c}\right)^5 - 15\left(\frac{X_c}{L_c}\right)^4 + 10\left(\frac{X_c}{L_c}\right)^3\right] \tag{3.1}$$

- Y_c: dependent variable (path)
- X_c: independent variable (length values)
- Y_{ci}: inlet half value of diameter, height or width.
- Y_{co}: outlet half value of diameter, height or width.
- L_c: length of contraction.

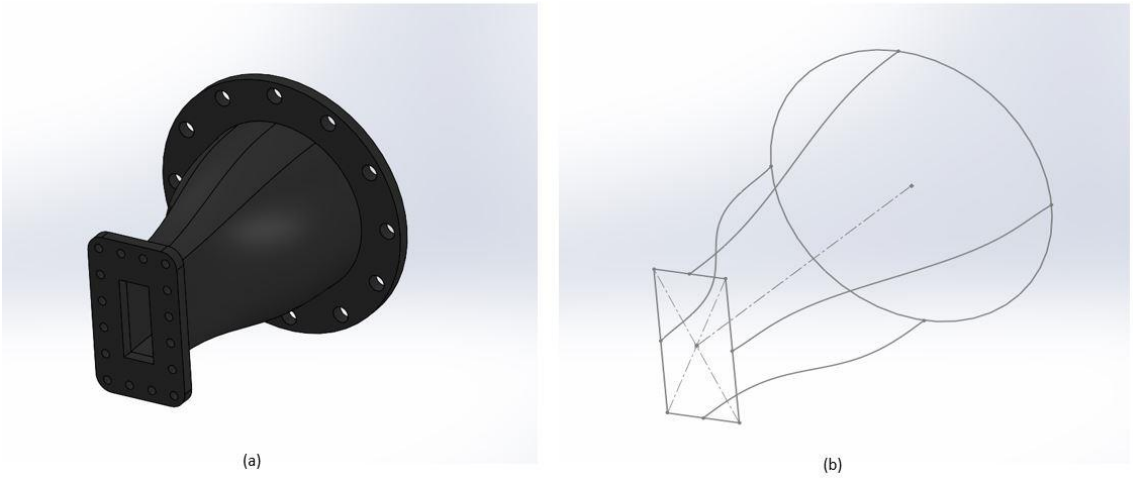

Figure 10 - (a). 5th order polynomial contraction. (b). Sketch of contraction with the 5th order polynomial path on the top, bottom, left, and right.

The 5^{th} order polynomial contraction 3D CAD model was made using SolidWorks software, as shown in Figure 10. The parametric equations make use of Eq. (3.1) to create the curvature path which was used in conjunction with the loft feature to create the complex geometry

3.3 Expansion

In this experimental facility two expansions can be found. The first connects the 6 inch piping to the 10 inch, with both having a circular cross section. The second connects the test section with the 8 inch piping. Therefore, it goes from a rectangular cross section to a circular one. Since the inlet and outlet geometries of both expansions are already known, the length is the only parameter that needs to be determined. This parameter is very important since if the expansion is too short, flow separation can occur. Moreover,

in order to avoid this phenomenon from occurring, the half angle parameter $\left(\phi_{\frac{1}{2}}\right)$ needs to be defined which is simply a function of geometry and defined as [17]:

$$\phi_{\frac{1}{2}} = \tan\left(\frac{D_{oe} - 2r_{eff}}{2L_e}\right) \tag{3.2}$$

This half angle equation is a function of the length (L_e), outlet diameter (D_{oe}), and the effective radius (r_{eff}) of the expansions. The effective radius has to be defined for both circular and rectangular inlets. For circular inlets the effective radius is simply the radius of the inlet. For rectangular geometry it can easily be derived by equating the area of a generic rectangle $(a \cdot b)$ and a circle.

$$a \cdot b = \pi r_{eff}^2 \tag{3.3}$$

$$r_{eff} = \sqrt{\frac{ab}{\pi}} \tag{3.4}$$

According to studies by [16], for conical expansions, flow separation was observed in half angles of 5° and for rectangular conduits with half angles of 4°. The expansions in the current study were design with length of 48 and 36 inches to achieve a half angle below the values stated above as shown in Table 3.1.

Table 2 - Expansions half angle values.

Expansion	Geometry	$\boldsymbol{\phi_{\frac{1}{2}}}$
Long (48”)	Circular to Circular (Conical)	4.16°
Short (36”)	Rectangular to Circular (Rectangular Conduit)	3.51°

Similar to the contraction, both expansions were made in SolidWorks as shown in Figure 11.

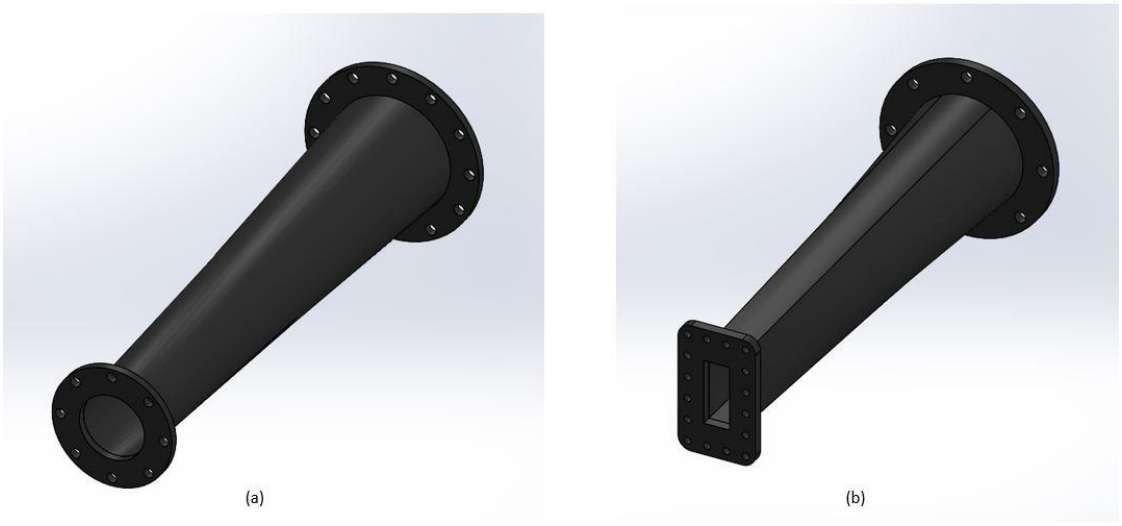

Figure 11 - (a). Long expansion. (b). Short expansion.

The parameters defined and used to design the expansion and contraction will be used to calculate the pressure drop and head loss of these components as it is shown in Chapter 4. Components such as the test section and the rest of the pipe system will also be covered in Chapter 4 along with system head loss curve and pump sizing.

4 SYSTEM HEAD LOSS & PUMP SIZING

4.1 General Overview

In order to select the size of the pump, a total system pressure drop or head loss must be determined. The head loss of the previously mentioned components must be calculated in order to quantify the operating point and possible flow rates this facility can achieve. An overview of the theory and derivations for all of the components will be provided in this chapter along with an analysis of the system curve of the facility and the performance curve of the pump. The general equation used to compute the total system pressure drop or head loss is in Eq. (4.1). The major losses are defined as any loss due to friction in a pipe system or channel. For this facility, the minor losses consist of elbow, reducers and contractions.

$$h_{L,total} = \sum_i f_i \frac{L_i}{D_i} \frac{V_i^2}{2g} + \sum_j K_{L,j} \frac{V_j^2}{2g} \tag{4.1}$$

4.2 Test Section Head Loss

As described in Chapter 2, the test section is composed of three channels. The first channel refers to the two identical side channels, channel two is the middle channel or bypass gap, and channel three is the channel based on the overall cross section. Since the fluid will be kept at a constant temperature, no changes in the density are expected.

Because of this, the conservation of mass can be expressed by volumetric flow balance as shown in Eq. (4.2).

$$Q_3 = 2Q_1 + Q_2 \tag{4.2}$$

It should be noted that $Q_3 = Q_{total}$, which equals to the operating volumetric flow rate of the experimental facility. Moreover, the pressure drop through channel 1 and 2 is identical since these flow paths are in parallel. The following general equation was used to determine the pressure drop across the two channels. It should be noted the use of Eq (4.3) applies for fully developed flow which was an assumption that was made to simplify the pressure drop calculation in the test section.

$$P_{ch} = \frac{\rho f_{ch} u_{ch}^2 L_p}{2D_{hch}} \tag{4.3}$$

For flow problems through parallel piping or channels, a typical solution strategy is to solve a system of equations as a function of the total flow rate entering the pipe system. The alternate approach used here was to determine the flow rates among the two zones. A flow rate in zone one will be assumed which will allow determination of the Reynolds number and friction factor, which can be determined with the following equations.

$$Re = \frac{uD}{\nu} \tag{4.4}$$

$$f_L = \frac{64}{Re}, \quad Re \leq 2300 \tag{4.5}$$

$$f_T \cong \left(-1.8\log\left[\frac{6.9}{Re}+\left(\frac{\varepsilon/D}{3.7}\right)^{1.11}\right]\right)^{-2}, \quad Re \geq 4000 \tag{4.6}$$

Equation (4.6) is an explicit formed given by S.E. Haaland in 1983 and results showed to be within 2% of the values obtained by the implicit Colebrook equation. For flow in the transition region between laminar and turbulent regimes, the following equations can be used.

$$r_{re} = \frac{Re - 2300}{4000 - 2300} \tag{4.7}$$

$$f_{mix} = (1 - r_{Re})f_L + r_{re}f_T \tag{4.8}$$

Using the equations stated above, the pressure drop across channel 1 can be determined. Since the pressure drop in channel 1 is identical to channel 2 the velocity in channel 2 can be determined by the following equation based on the same assumptions in Eq. (4.3).

$$u_{ch2} = \sqrt{\frac{2P_{ch1}D_{hch2}}{\rho f_{ch2}L_p}} \tag{4.9}$$

In order to use Eq (4.8), the friction factor f_{z2} must be determined but since it is a function of the Reynolds number it is also a function of the velocity therefore a guess value of the friction factor is needed. The following algorithm is used to reach the true value of u_{ch2}.

1. Define a value for f_{guess} and the value for ϵ (condition for iterative convergence).
2. Replace the friction factor in Eq. (4.9) with the value guessed in step 1.
3. Calculate the Reynolds number with the value obtained from step 2.

4. Calculate the new friction factor (f_{new}) using Eq. (4.5), (4.6), or (4.7) depending on the flow regime.
5. Calculate the difference between the guess and new friction factor:

   $\epsilon = |f_{new} - f_{guess}|$.
6. Set $f_{guess} = f_{new}$ and repeat steps 2-6 until $\epsilon < 10^{-5}$.

Through this iterative procedure, the velocity for channel 2 is determined, and the volumetric flow rate can easily be calculated. This enables use of Eq. (4.1) and (4.2) to determine the flow rate and pressure drop in channel 3. The total pressure drop and head loss are giving in Eq. (4.10) and (4.11).

$$\Delta P_{ts} = \Delta P_{ch1} + \Delta P_{ch3} \tag{4.10}$$

$$h_{ts} = \frac{\Delta P_{ts}}{\rho g} \tag{4.11}$$

4.3 Contraction Head Loss

The contraction pressure drop was modeled as a sudden contraction and it was treated as a minor loss due to the complex geometry in order to simplify calculations. Any discrepancies in the pressure drop from this assumption are taken into account with the pump selection. The pressure drop was calculated using the equation below.

$$h_c = K_{Lc} \frac{V_{avg}^2}{2g} \tag{4.12}$$

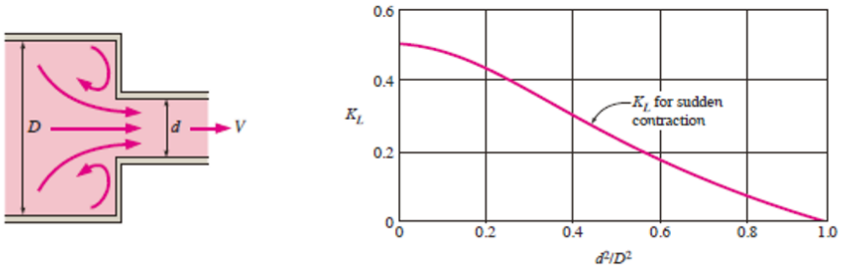

Figure 12 - Minor loss coefficient for sudden contraction [1].

The value for K_{Lc} was obtained by dividing the outlet of the contraction by the inlet diameter and squaring the ratio. Since the outlet of the contraction has a rectangular cross section, Eq. (3.4) was used and multiplied by two to get the effective diameter. The ratio $\frac{2r_{eff}^2}{D_{ci}^2}$ has a value of 0.127. Referring to Figure 12, on the horizontal axis, the value 0.127 corresponds to a value of approximately 0.5. Therefore, a K_{Lc} value of 0.5 was used as the minor loss coefficient.

4.4 Expansion Head Loss

The expansion pressure drop is determined by a straightforward derivation as showed in Ripken [16]. Figure 13 below shows the variables that describe the geometrical parameter of the expansion which are used for the derivation. By definition the head loss in a pipe can be expressed as shown in Eq. (4.13).

$$h_e = \frac{f V_{avg}^2 L}{2dg} \tag{4.13}$$

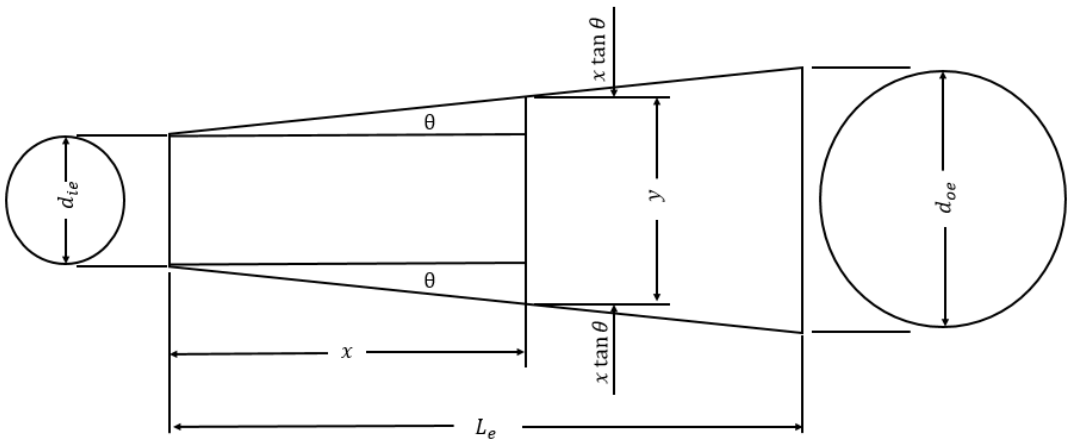

Figure 13 - Expansion geometrical diagram.

In order to account for the variable geometry Eq. (4.11) needs to be expressed as:

$$dh_e = \frac{fV_{avg}^2}{2yg}dx \tag{4.14}$$

As showed in Figure xx, it can be seen that $y = d_{ie} + 2x\tan\theta$. Note that $\theta = \phi_{\frac{1}{2}}$. Furthermore, $dx = \frac{dy}{2\tan\theta}$. In general terms Eq. (4.12) becomes:

$$dh_e = \frac{fV_{avg}^2}{4\tan\theta}\frac{dy}{y} \tag{4.15}$$

From a mass balance with constant density we can arrive to an expression that relates the average squared velocity at any point (V_{avg}^2) to the inlet average velocity ($\bar{V}_{ie}^2$). This expression is shown in Eq. (4.16).

$$V_{avg}^2 = \bar{V}_{ie}^2\left(\frac{d_{ie}}{y}\right)^4 \tag{4.16}$$

Rearranging the terms in Eq. (4.15) yields the following:

$$h_e = \frac{f\bar{V}_{ie}^2 d_{ie}^4}{4g\tan\theta}\int_{d_{ie}}^{d_{oe}} \frac{dy}{y^5} \tag{4.17}$$

Lastly, the head loss and pressure drop in the expansion can be determined.

$$h_e = \frac{f\bar{V}_{ie}^2 d_{ie}^4}{16g\tan\theta}\left[\frac{1}{d_{ie}^4} - \frac{1}{d_{oe}^4}\right] \tag{4.18}$$

4.5 Pipe and Fittings Head Loss

As mentioned before, the pipe system consists of schedule 10 piping. Referring to Figure 5 and Figure 6 will be helpful to comprehend the MIR facility pipe system. Starting from the pump's outlet, an 8-inch nominal to 6-inch nominal reducer is connected. The 6-inch nominal side of the reducer connects to a 6×6×2 tee which is connected to a straight 49.5-inch long 6-inch nominal pipe. This straight pipe then connects to another 6×6×2 tee. The 6-inch pipe section combined has a length of 86 inches. In this section the two tees are used as drain ports. Following the long expansion, a 10-inch nominal long radius elbow is found which connects to a straight 15-inch long pipe which then followed by the flow conditioner and 38-inch long settling chamber. After the 10-inch nominal piping, the contraction, test section, and short expansion, the 8-inch nominal piping commences which is the return leg to the inlet of the pump. The return leg consists of an 8×8×3 tee which is the filling port of the facility, an 8-inch 90-degree long radius elbow which connects to a 20 inch long vertical straight pipe which lead to an another elbow and lastly a 19.5 inch long horizontal straight pipe that connects to the pump's inlet. The head loss

was calculated using Eq. (4.1) which requires the identification of the major and minor losses in the system. Table 3 classifies each component and provides information on the head loss coefficient.

Table 3 - Component Classification

Component	Type of Loss	K_L
Straight Pipe	Major	N/A
Elbow	Minor	0.3
Flow Conditioner	Minor	0.3
Reducer	Minor	0.04
Tee	Major	N/A

The minor loss coefficient can be found from any Fluid Mechanics book and from many sources. The information provided in Table 3 was obtained from [1] Although the flow conditioner has internal turning vanes, it was assumed to be an elbow in order to simplify calculating the system curve. All of these assumptions are considered when selecting the pump for the system.

4.6 Total Pressure Drop and Pump Selection

The total pressure drop as a function of flow rate was calculated using the information found in the previous sections. The pump that was selected for this system is an Armstrong Fluid Technology Design Envelope 4300 Vertical In-line Pump Unit. The

pump is rated at 20 hp (horsepower) and has an 8.13-inch impeller. The manufacturer specifications include the pump curves which suggest pressures and flow ranges at desirable levels and at high efficiency operating points. The pump is also equipped with variable frequency drive (VFD) which allows for further customization of the pump's performance curve to further ensure the targeted flow rate is met. Figure 14 illustrates the system curve along with different operating curves at different frequencies and efficiency curves which were provided by the manufacturer. Furthermore, there is an asterisk which indicates the minimum operating flow conditions to achieve the target Reynolds number of 10^4 in channel 2.

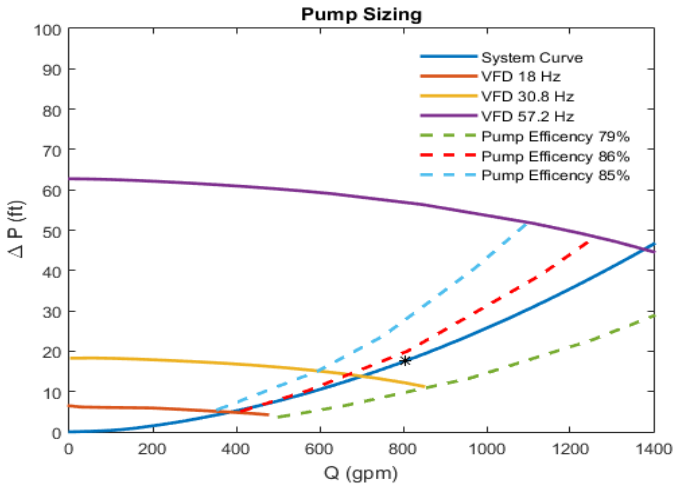

Figure 14 - System pressure drop and pump sizing.

Referring to Figure 14, the three dash lines represent the pump's operating efficiency. It can be seen that the system curve is in between the red dashed line and the green dashed line which represents an operating efficiency between 86% and 79%. Having a system curve to the left of the blue dash line (85%) will cause the pump's efficiency to decrease similarly having the system curve to the right of the green dash line. Moreover, it is

expected that the system curve will remain close to what it is shown in Figure 14. As for the pump's operating frequency, it is expected to be between 30.8 Hz and 57.2 Hz or close to 40 Hz. Having the ability to manipulate the pump's operating point was an important specification when selecting the pump which will allow us to explore different test section geometries and future modifications to the MIR facility as will be discussed in Chapter 5.

5 FUTURE WORK AND CONCLUSION

For future work, there are some improvements that can be made for the MIR facility. These improvements will allow for the testing of other geometries in the test section and also to facilitate the necessary changes to the system. One of the most prominent of these modifications is the substitution of an alternative design for test section 1. As shown in Figure 15, this alternative design consists of manufacturing a stainless steel or aluminum frame and welding it together. The frame will have threaded holes along the top, bottom, and sides for placement of acrylic windows with gaskets which will form a seal against the framing.

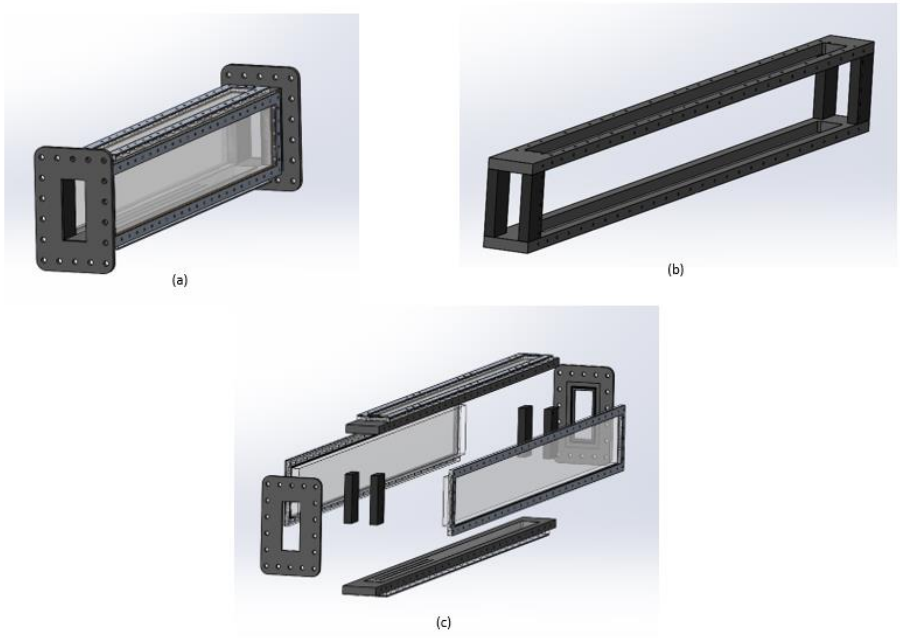

Figure 15 - Alternative test section design: (a) isometric assembly view (b) test section frame, and (c) exploded view.

The alternative test section design will allow for the removal of the acrylic windows without having to dismount the test section from the facility. This will facilitate changes for different geometries and studies of interest. Figure 16 shows a detailed view of the top/bottom frame and window assembly.

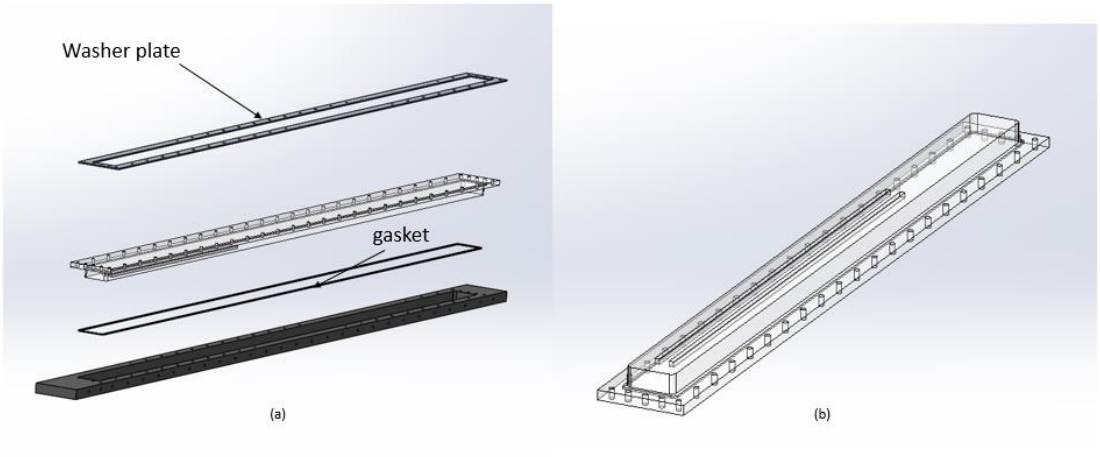

Figure 16 - (a) Top/bottom window assembly. (b) Top/bottom acrylic window with grooves.

In order to acquire further knowledge in turbulent mixing across narrow channels, different test section channel sizes should be studied in the future. Referring to Figure 7a from chapter 1, the ratio of t_1 to t_2 is called the delta ratio as shown in Eq. (5.1)

$$\delta_r = \frac{t_1}{t_2} \tag{5.1}$$

The current test section design has a delta ratio of 1.5. However, a wide range of this parameter is of potential interest when considering next generation nuclear reactors. To fully explore the flow physics of this mixing problem, the facility should enable ease of switching test sections of different geometries in and out. The alternative test section will simplify this process compared to the current design. To accomplish this, the top and bottom windows are removed along with the quartz plates and the new top bottom windows with the desired groove spacing would be installed. This design would reduce costs and time when doing such modifications with the downfall of being more expensive upfront in comparison to the full acrylic test section. It should be mentioned that this alternative design would have the same interior dimensions and length as the current design. Detailed dimensions and drawings of this design can be found in the appendix along with drawings for the current test section design.

The last suggested modification that will be discussed is the addition of a secondary cooling loop. Since this is a recirculating loop, any heat produced by the pump will be transferred to the surroundings and to the mineral oil for this application. The heating of the mineral oil of the system can have a negative effect when gathering data since the index of refraction of the fluid is a function of the temperature. At the moment, the amount of heat that will need to be removed from the system is still unknown since more testing must be done in order to acquire the necessary data to determine the pump's energy transfer to the mineral oil. Similar to the INL MIR facility cooling system, a secondary loop should be implemented for this MIR facility. The secondary loop would

connect to the two drain ports or the two 6×6×2 tees. This loop would consist of a simple pipe system that feeds off the main loop taking a portion of the mineral oil. This pipe system will be connected to a closed feed heat exchanger which then connects to the second tee downstream before the long expansion. The cold side of the heat exchanger will be connected to a chiller that will remove the necessary heat generated from the pump. The secondary tee will recombine the incoming cold mineral from the secondary loop and the hot mineral oil from the primary. Heaters and a control system could also be added which would help to maintain the mineral oil at a constant temperature.

Although the design and construction of experimental facility was accomplished, some problems were encountered and solved. The used of gaskets for raised face flanges prove to be troublesome in a few occasions. Since a gasket sealant was necessary in order to hold the gasket in place, it sometimes did not dry correctly in certain locations and made the gasket slip which resulted in an improper seal. The solution to fix this problem was to use full face flange gaskets which have bolt holes. The bolt holes in the gasket allowed for a good placement of the gasket in between the two type of flanges (raised and flat face) and prevented the gasket from slipping. Another problem that occurred were the slight difference in length of piping pieces. This resulted in a 0.5 inch gap between the final pieces in bottom piping, and was addressed through installation of a thick polycarbonate spacer which was machined to have the dimensions of the flange. The most important lesson learned from assembling the facility is to start construction once that pump is placed or fixed. Since the pump is the heaviest object in the system, it acts like an anchor. Any

adjustment in the piping system or the test section becomes very difficult because the pumps prevents other components from moving. Having the pump installed first will allow each component to fall in its place resulting in less time with leveling adjustments. Although it was difficult to make changes and alignments in the system, the test section is within 0.5° with the horizontal. Lastly, the facility was filled with mineral oil and all leaks were addressed and fixed. Although the facility has not been tested due to delays of the electrical connection of the pumps, it is hoped that this experimental facility will allow for further understanding of turbulent mixing along with other physical phenomena that may be of interest in future studies.

REFERENCES

[1] J. M. C. Yanus A. Cengel, *Fluid Mechanics Fundamentals and Applications*: McGraw Hill, 2006.

[2] P. E. MacDonald, A. Baxter, P. Bayless, J. Bolin, H. Gougar, R. Moore, *et al.*, "The Next Generation Nuclear Plant-Insights gained from the INEEL Point Design Studies," Idaho National Laboratory (INL)2004.

[3] S. Salkhordeh, "Large Eddy Simulations of isothermal and non-isothermal turbulent flows for High Temperature Gas Cooled Reactors," University of Pittsburgh, 2015.

[4] S. Salkhordeh, C. Clifford, A. Jana, and M. L. Kimber, "Large Eddy Simulations of scaled HTGR lower plenum for assessment of turbulent mixing," *Nuclear Engineering and Design*, vol. 334, pp. 24-41, 2018.

[5] L.-W. Hu, "LES benchmark study of high cycle temperature fluctuations caused by thermal striping in mixing teeq," *International Journal of Heat and Fluid Flow*, vol. 27, 2006.

[6] A. Clayton, "Thermal shock in nuclear reactors," *progress in nuclear energy*, vol. 12, pp. 57-83, 1983.

[7] G. Lloyd and D. Wood, "Fatigue crack initiation and propagation as a consequence of thermal striping," *International Journal of Pressure Vessels and Piping*, vol. 8, pp. 255-272, 1980.

[8] A. Tokuhiro and N. Kimura, "An experimental investigation on thermal striping: Mixing phenomena of a vertical non-buoyant jet with two adjacent buoyant jets

as measured by ultrasound Doppler velocimetry," *Nuclear Engineering and Design,* vol. 188, pp. 49-73, 1999.

[9] Q. Cao, D. Lu, and J. Lv, "Numerical investigation on temperature fluctuation of the parallel triple-jet," *Nuclear Engineering and Design,* vol. 249, pp. 82-89, 2012.

[10] S. B. Rodriguez and M. S. El-Genk, "Numerical investigation of potential elimination of 'hot streaking'and stratification in the VHTR lower plenum using helicoid inserts," *Nuclear Engineering and Design,* vol. 240, pp. 995-1004, 2010.

[11] S. B. Rodriguez, S. Domino, and M. S. El-Genk, "Fluid Flow and Heat Transfer Analysis of the VHTR Lower Plenum using the Fuego CFD Code," *CFD4NRS-3, Nuclear Regulatory Commission, Bethesda, MD,* 2010.

[12] C. Betts, C. Boorman, and N. Sheriff, "Thermal striping in liquid metal cooled fast breeder reactors," in *Thermal hydraulics of nuclear reactors*, ed, 1983.

[13] N. Kimura, H. Miyakoshi, and H. Kamide, "Experimental investigation on transfer characteristics of temperature fluctuation from liquid sodium to wall in parallel triple-jet," *International Journal of Heat and Mass Transfer,* vol. 50, pp. 2024-2036, 2007/05/01/ 2007.

[14] S. Mazumdar, D. Landfried, A. Jana, and M. Kimber, "Initial Computational Study of The Thermal Mixing In A VHTR Lower Plenum," in *NURETH 15-608, 15th International Topical Meeting on Nuclear Reactor Thermal hydraulics,* 2013, pp. 12-15.

[15] D. Tenchine, "Some thermalhydraulic challenges in sodium cooled fast reactors," *Nuclear Engineering and Design,* vol. 240, 2010.

[16] J. F. Ripken, "Design Study for a Closed-Jet Water Tunnel " *University of Minnesota, St. Anthony Falls Hydraulics Laboratory* vol. Technical Paper No 9, Series B 1951.

[17] I. Nedyalkov, "Design of Contraction, Test Section, Diffuser for a High-Speed Water Tunnel " Master of Science Department of Applied Mechanics, Chalmers University of Technology 2012.

[18] L. Daniel, "Design and Installation of a High Reynolds Number Recirculating Water Tunnel," Master of Science, Aerospace Engineering, Oklahoma State University, UMI Dissertation Publishing 2014.

[19] J. Hugh M. Mcllroy, Donald M. McEligot, Richard R. Schultz, Daniel Christensen, Robert J. Pink, Ryan C. Johnson "PIV Experiments to Measure Flow Phenomena in a Sacaled Model of a VHTR Lower Plenum," *Idaho National Laboratory,* 2006.

[20] R. D. M. J. H. Bell, "Contraction Design for Small Low-Speed Wind Tunnels " *National Aeronautics and Space Administration,* 1988.

APPENDIX

Manufactures and Distributors:

Manufacture	Distributor	Part	Part Number
Moore Fabrication	Moore Fabrication (Houston TX)	Test Section	N/A
Armstrong Fluid Technology	Texas Air System Houston	Centrifugal Inline Pump	751196-364
Newport Corporation	Newport Corporation	Optical Table	N/A
Stockwell Elastomerics, INC.	Stockwell Elastomerics, INC.	Test Section Gaskets	N/A
TW Metals	TW Metals	Schedule 10 Piping	N/A
Vortab	Alpha Process Sales, INC.	Flow Conditioner	C084790-1
Penreco	Calumet Refining, LLC	Drakeol 5LT Mineral Oil	N/A
McMaster	McMaster	Miscellaneous	N/A
Diehl Aero-Nautical Co.	Diehl Aero-Nautical Co.	Contraction Expansions	N/A

Test Section Drawings

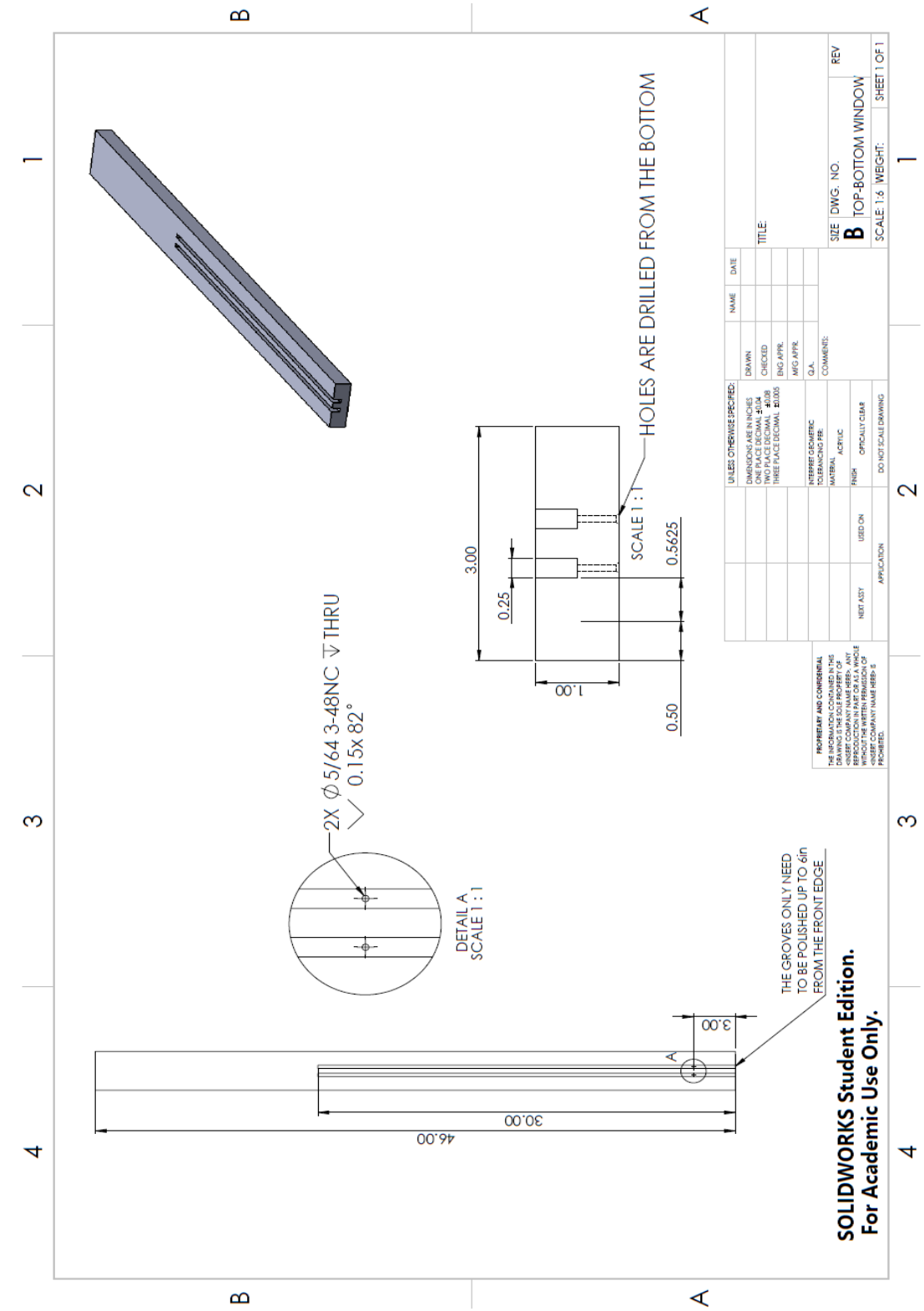

SCALE 1 : 10

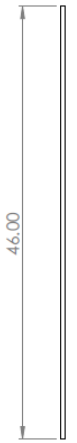

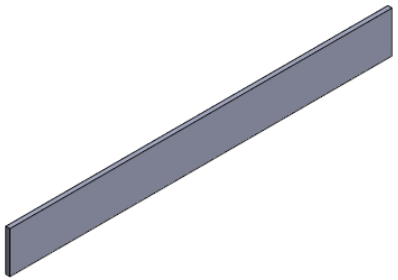

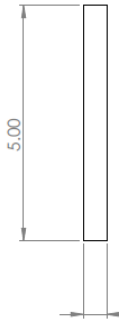

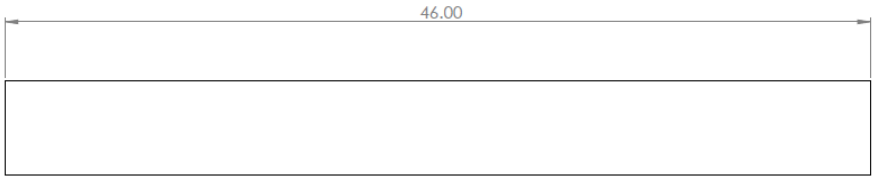

SOLIDWORKS Student Edition.
For Academic Use Only.

		UNLESS OTHERWISE SPECIFIED:		NAME	DATE
		DIMENSIONS ARE IN INCHES TOLERANCES: ONE PLACE DECIMAL ± 0.08 TWO PLACE DECIMAL ± 0.04 THREE PLACE DECIMAL ± 0.005	DRAWN		
			CHECKED		TITLE:
			ENG APPR.		
			MFG APPR.		
		INTERPRET GEOMETRIC TOLERANCING PER:	Q.A.		
		MATERIAL ACRYLIC	COMMENTS:		SIZE B / DWG. NO. Side Window / REV
NEXT ASSY	USED ON	FINISH OPTICALLY CLEAR			
APPLICATION		DO NOT SCALE DRAWING			SCALE: 1:5 / WEIGHT: / SHEET 1 OF 1

PROPRIETARY AND CONFIDENTIAL

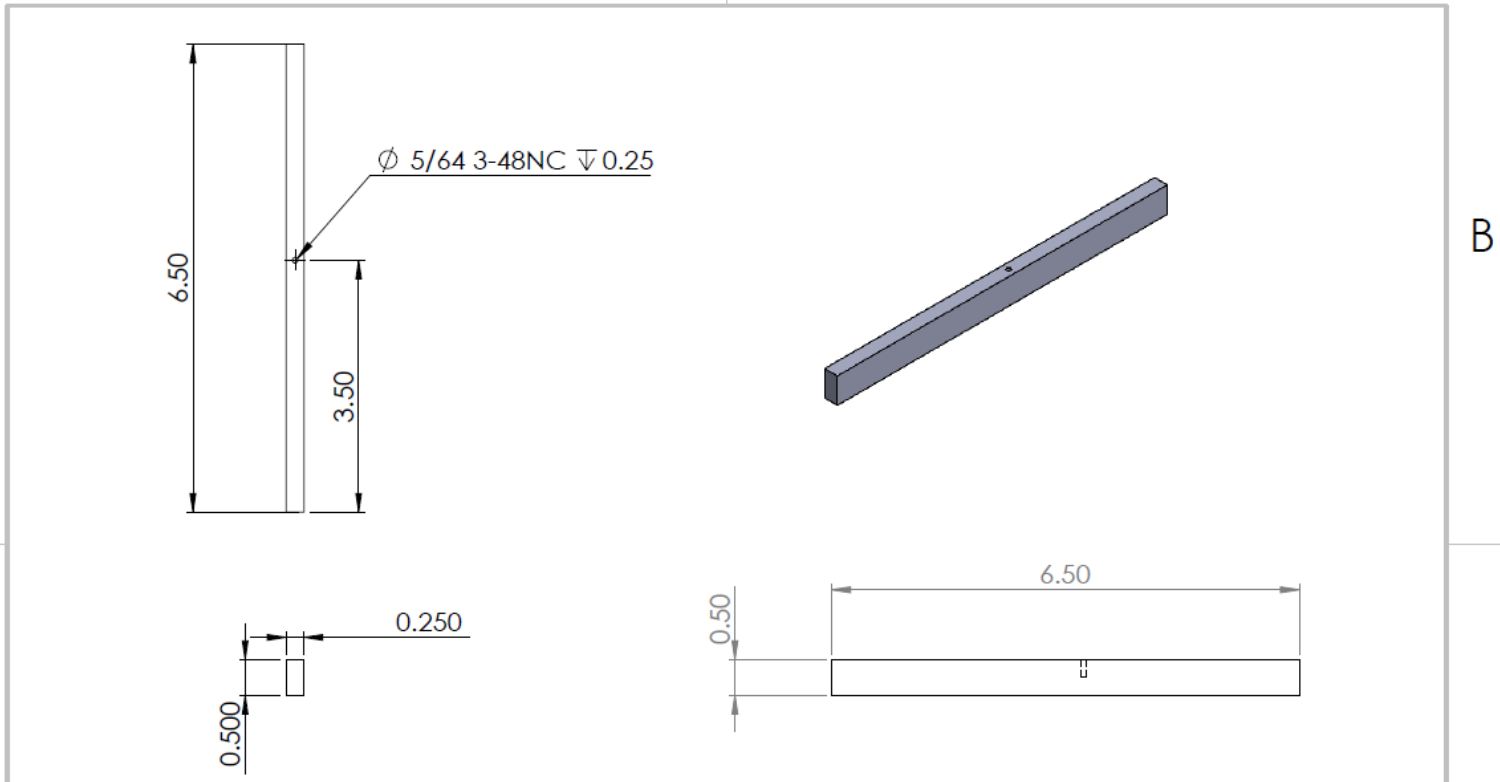

FRONT

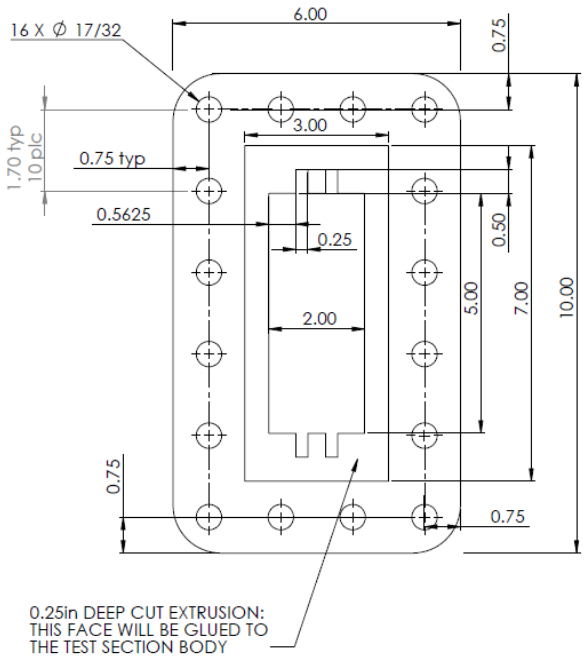

BACK

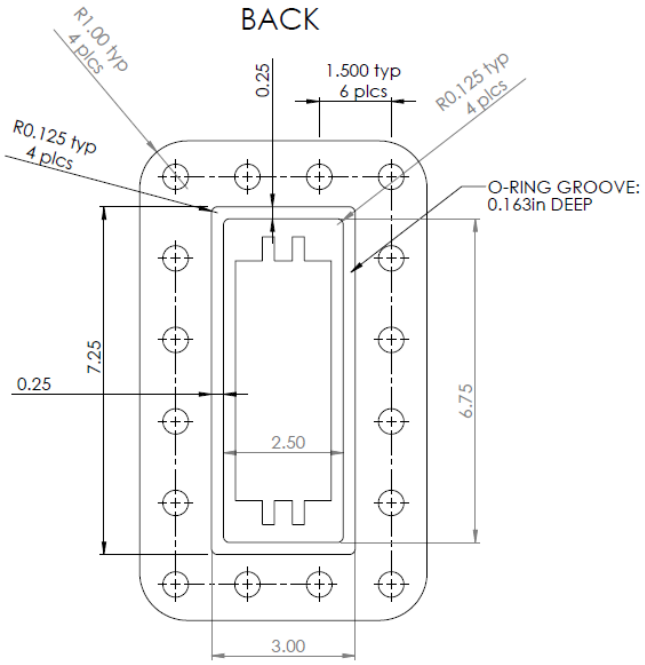

3D CAD MODEL IS PROVIDED FOR FURTHER CLARIFICATION

FLANGE THICKNESS: 0.75in.

SOLIDWORKS Student Edition.
For Academic Use Only.

		UNLESS OTHERWISE SPECIFIED:		NAME	DATE
		DIMENSIONS ARE IN INCHES ONE PLACE DECIMAL ± 0.08 TWO PLACE DECIMAL ±0.04 THREE PLACE DECIMAL ±0.005	DRAWN		
			CHECKED		
			ENG APPR.		
			MFG APPR.		
		INTERPRET GEOMETRIC TOLERANCING PER:	Q.A.		
		MATERIAL ACRYLIC	COMMENTS:		
NEXT ASSY	USED ON	FINISH GROUND FINISH			
APPLICATION		DO NOT SCALE DRAWING			

TITLE:

SIZE	DWG. NO.	REV
B	FLANGE: MODEL A	

SCALE: 1:2 | WEIGHT: | SHEET 1 OF 1

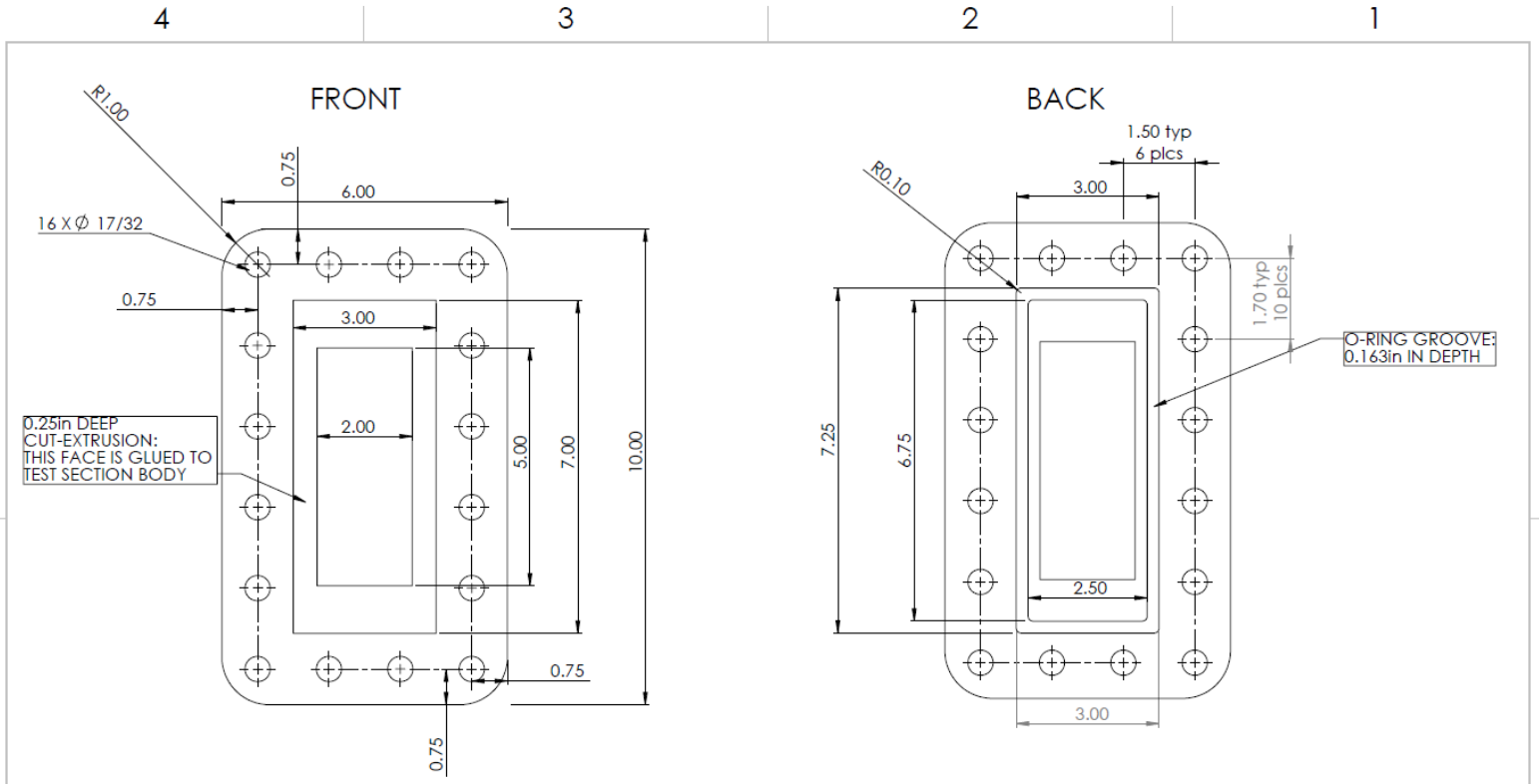

SAME AS MODEL A BUT WITHOUT INSEART SLOTS

FLANGE THICKNESS: 0.75in.

SOLIDWORKS Student Edition.
For Academic Use Only.

		UNLESS OTHERWISE SPECIFIED:		NAME	DATE
		DIMENSIONS ARE IN INCHES ONE PLACE DECIMAL ± 0.08 TWO PLACE DECIMAL ±0.04 THREE PLACE DECIMAL ±0.005	DRAWN		
			CHECKED		
			ENG APPR.		
			MFG APPR.		
		INTERPRET GEOMETRIC TOLERANCING PER:	Q.A.		
		MATERIAL ACRYLIC	COMMENTS:		
NEXT ASSY	USED ON	FINISH GROUND FINISH			
APPLICATION		DO NOT SCALE DRAWING			

TITLE:

SIZE	DWG. NO.	REV
B	FLANGE MODEL: B	

SCALE: 1:2 | WEIGHT: | SHEET 1 OF 1

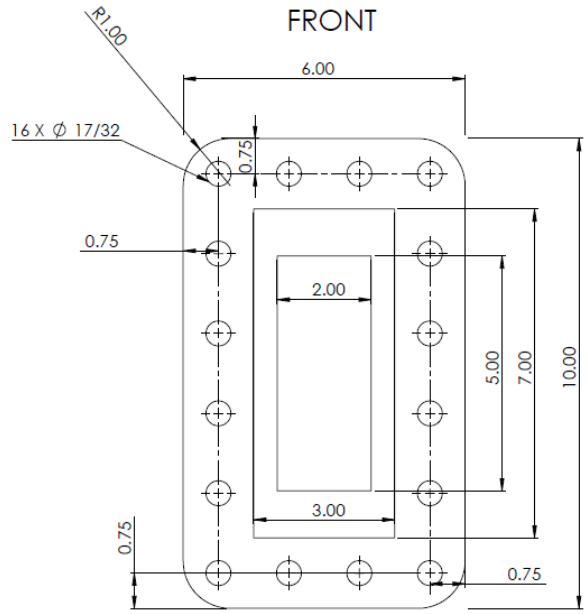

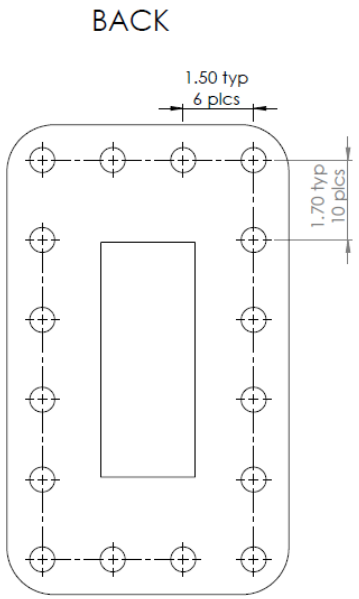

FLANGE THICKNESS: 0.75
NO INSEART SLOTS.
NO O-RING GROOVE.

SOLIDWORKS Student Edition.
For Academic Use Only.

		UNLESS OTHERWISE SPECIFIED:		NAME	DATE
		DIMENSIONS ARE IN INCHES ONE PLACE DECIMAL ± 0.08 TWO PLACE DECIMAL ± 0.04 THREE PLACE DECIMAL ± 0.005	DRAWN		
			CHECKED		
			ENG APPR.		
			MFG APPR.		
		INTERPRET GEOMETRIC TOLERANCING PER:	Q.A.		
		MATERIAL ACRYLIC	COMMENTS:		
NEXT ASSY	USED ON	FINISH GROUND FINISH			
APPLICATION		DO NOT SCALE DRAWING			

PROPRIETARY AND CONFIDENTIAL
THE INFORMATION CONTAINED IN THIS DRAWING IS THE SOLE PROPERTY OF <INSERT COMPANY NAME HERE>. ANY REPRODUCTION IN PART OR AS A WHOLE WITHOUT THE WRITTEN PERMISSION OF <INSERT COMPANY NAME HERE> IS PROHIBITED.

TITLE:

SIZE	DWG. NO.	REV
B	FLANGE MODEL C	
SCALE: 1:2	WEIGHT:	SHEET 1 OF 1

Alternative Test Section Drawings

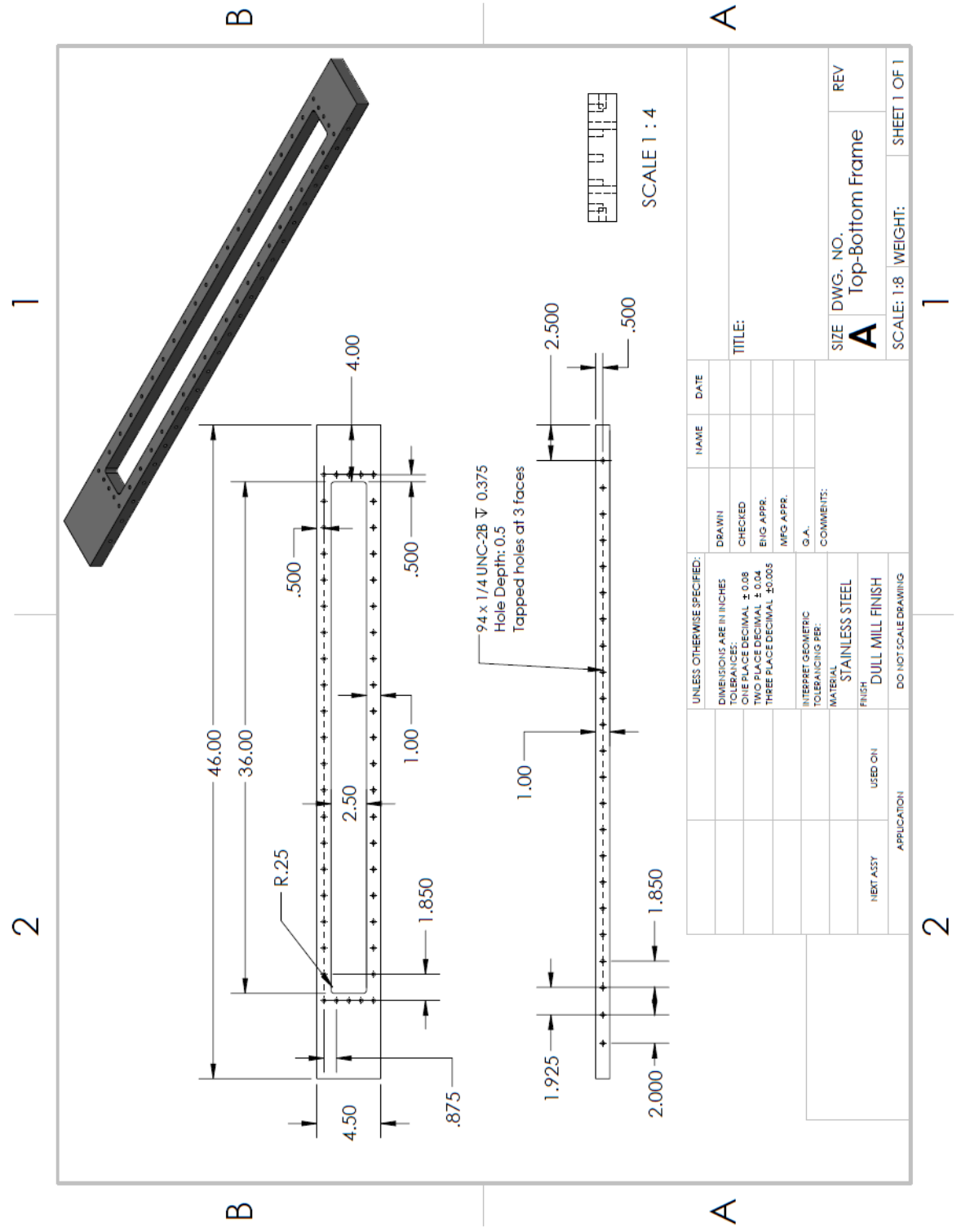

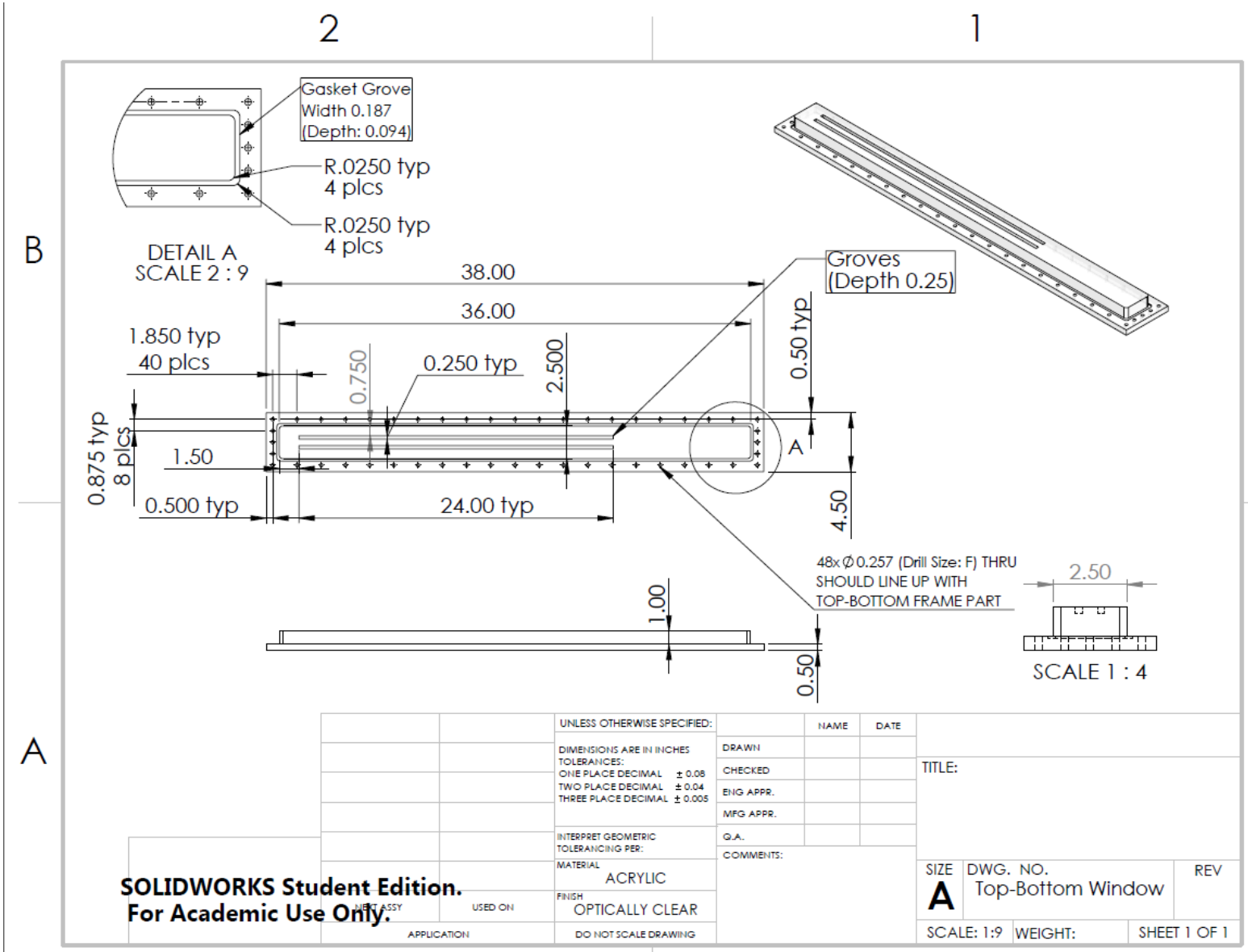
Gasket Grove
Width 0.187
(Depth: 0.094)
R.0250 typ
4 plcs
R.0250 typ
4 plcs
DETAIL A
SCALE 2 : 9
38.00
36.00
1.850 typ
40 plcs
0.750
0.250 typ
2.500
Groves
(Depth 0.25)
0.50 typ
0.875 typ
8 plcs
1.50
0.500 typ
24.00 typ
A
4.50
48x Ø0.257 (Drill Size: F) THRU
SHOULD LINE UP WITH
TOP-BOTTOM FRAME PART
1.00
0.50
2.50
SCALE 1 : 4
UNLESS OTHERWISE SPECIFIED:
DIMENSIONS ARE IN INCHES
TOLERANCES:
ONE PLACE DECIMAL ± 0.08
TWO PLACE DECIMAL ± 0.04
THREE PLACE DECIMAL ± 0.005
INTERPRET GEOMETRIC TOLERANCING PER:
MATERIAL
ACRYLIC
FINISH
OPTICALLY CLEAR
DO NOT SCALE DRAWING
NAME
DATE
DRAWN
CHECKED
ENG APPR.
MFG APPR.
Q.A.
COMMENTS:
TITLE:
SIZE
A
DWG. NO.
Top-Bottom Window
REV
SCALE: 1:9
WEIGHT:
SHEET 1 OF 1
NEXT ASSY
USED ON
APPLICATION
SOLIDWORKS Student Edition.
For Academic Use Only.

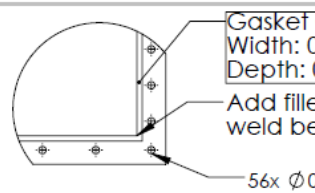

DETAIL A
SCALE 1 : 5

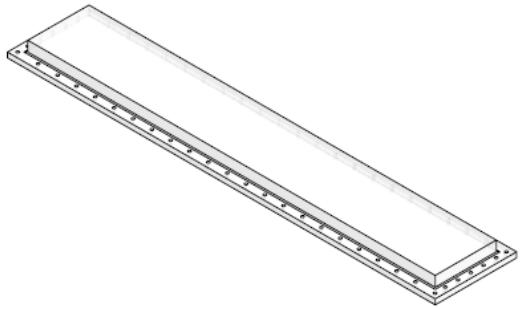

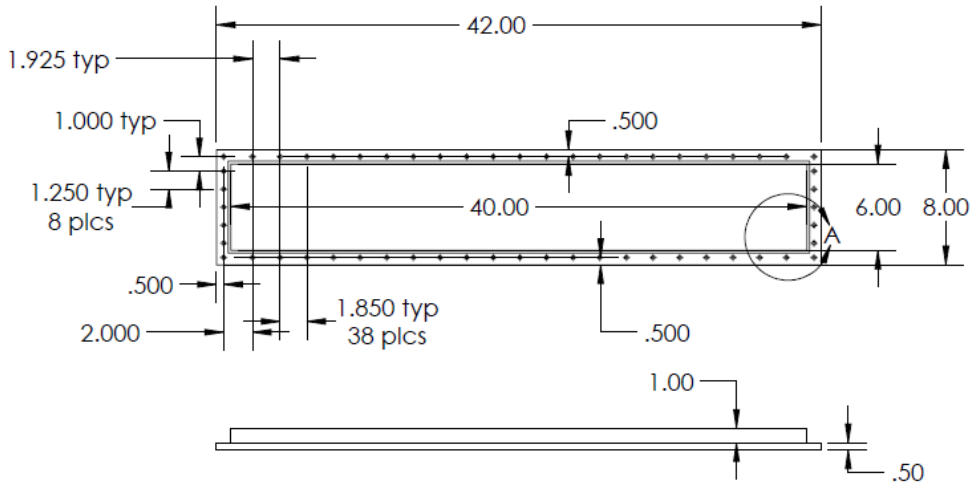

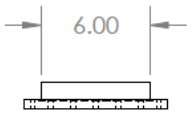

SCALE 1 : 8

		UNLESS OTHERWISE SPECIFIED:		NAME	DATE
		DIMENSIONS ARE IN INCHES TOLERANCES: ONE PLACE DECIMAL ± 0.08 TWO PLACE DECIMAL ± 0.04 THREE PLACE DECIMAL ± 0.005	DRAWN		
			CHECKED		
			ENG APPR.		
			MFG APPR.		
		INTERPRET GEOMETRIC TOLERANCING PER:	Q.A.		
		MATERIAL ACRYLIC	COMMENTS:		
NEXT ASSY	USED ON	FINISH OPTICALLY CLEAR			
APPLICATION		DO NOT SCALE DRAWING			

TITLE:

SIZE	DWG. NO.	REV
A	Side Window	
SCALE: 1:10	WEIGHT:	SHEET 1 OF 1

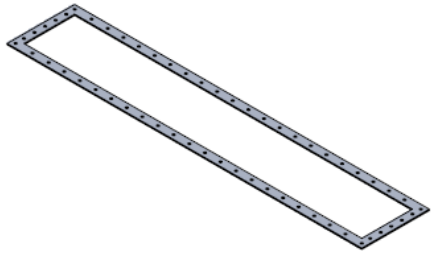

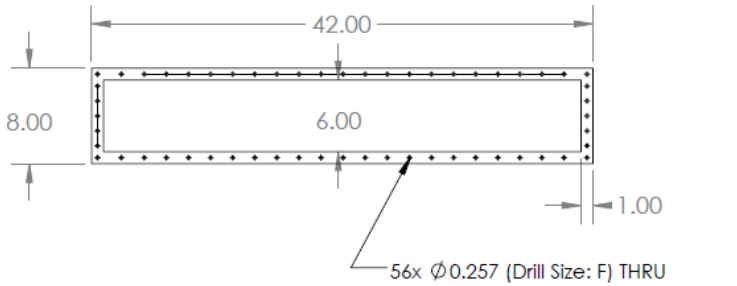

NOTE:
HOLE PATTERN IS THE SAME AS SIDE WINDOWPART

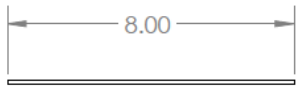

SCALE 1 : 4

		UNLESS OTHERWISE SPECIFIED:		NAME	DATE
		DIMENSIONS ARE IN INCHES TOLERANCES: ONE PLACE DECIMAL ± 0.08 TWO PLACE DECIMAL ± 0.04 THREE PLACE DECIMAL ±0.005	DRAWN		
			CHECKED		
			ENG APPR.		
			MFG APPR.		
		INTERPRET GEOMETRIC TOLERANCING PER:	Q.A.		
		MATERIAL ALUMINUM	COMMENTS:		
NEXT ASSY	USED ON	FINISH GROUND FINISH			
APPLICATION		DO NOT SCALE DRAWING			

TITLE:

SIZE	DWG. NO.	REV
A	SIDE WINDOW SHEET COVER	
SCALE: 1:12	WEIGHT:	SHEET 1 OF 1

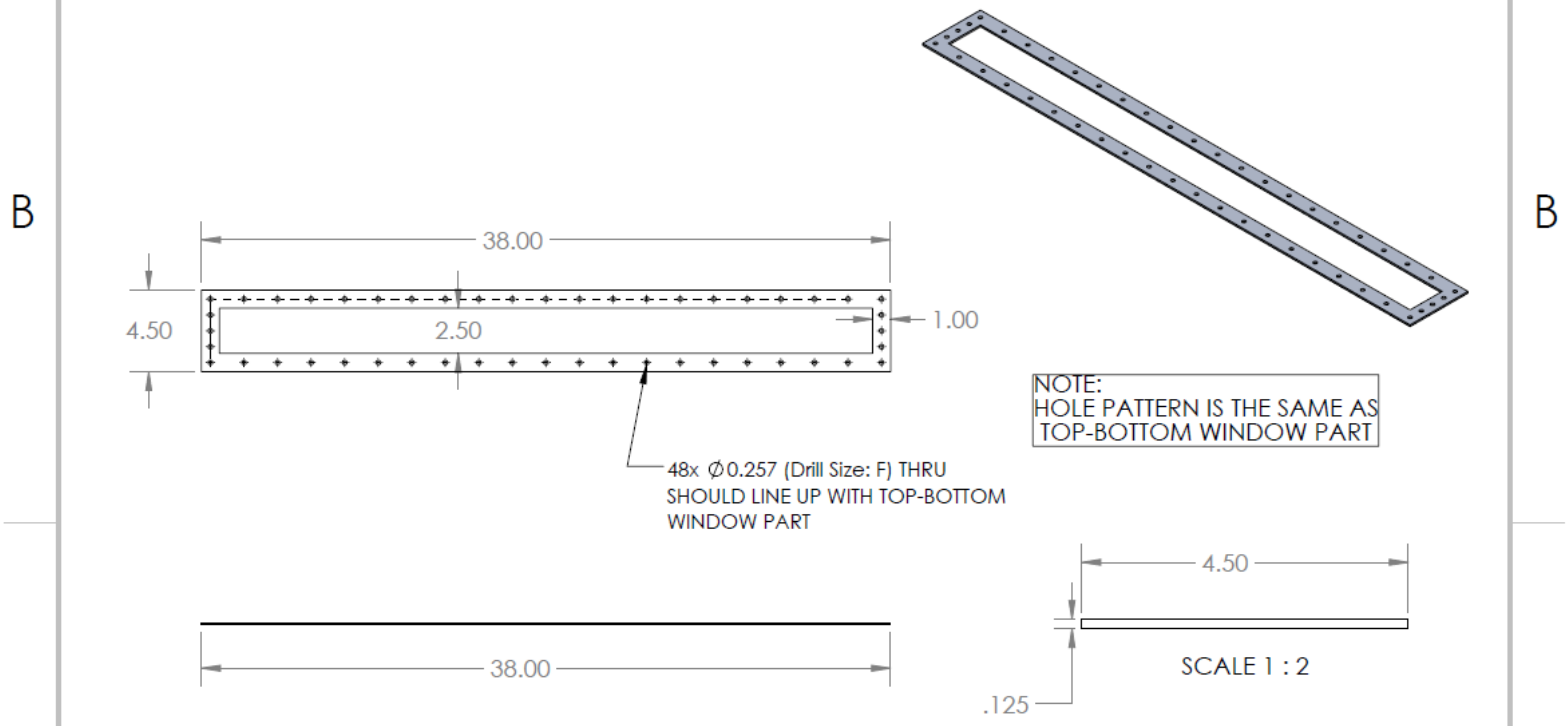

		UNLESS OTHERWISE SPECIFIED:		NAME	DATE
		DIMENSIONS ARE IN INCHES TOLERANCES: ONE PLACE DECIMAL ± 0.08 TWO PLACE DECIMAL ± 0.04 THREE PLACE DECIMAL ±0.005	DRAWN		
			CHECKED		
			ENG APPR.		
			MFG APPR.		
		INTERPRET GEOMETRIC TOLERANCING PER:	Q.A.		
		MATERIAL ALUMINUM	COMMENTS:		
NEXT ASSY	USED ON	FINISH GROUND FINISH			
APPLICATION		DO NOT SCALE DRAWING			

TITLE:

SIZE	DWG. NO.	REV
A	TOP-BOTTOM WINDOW SHEET COVER	
SCALE: 1:8	WEIGHT:	SHEET 1 OF 1

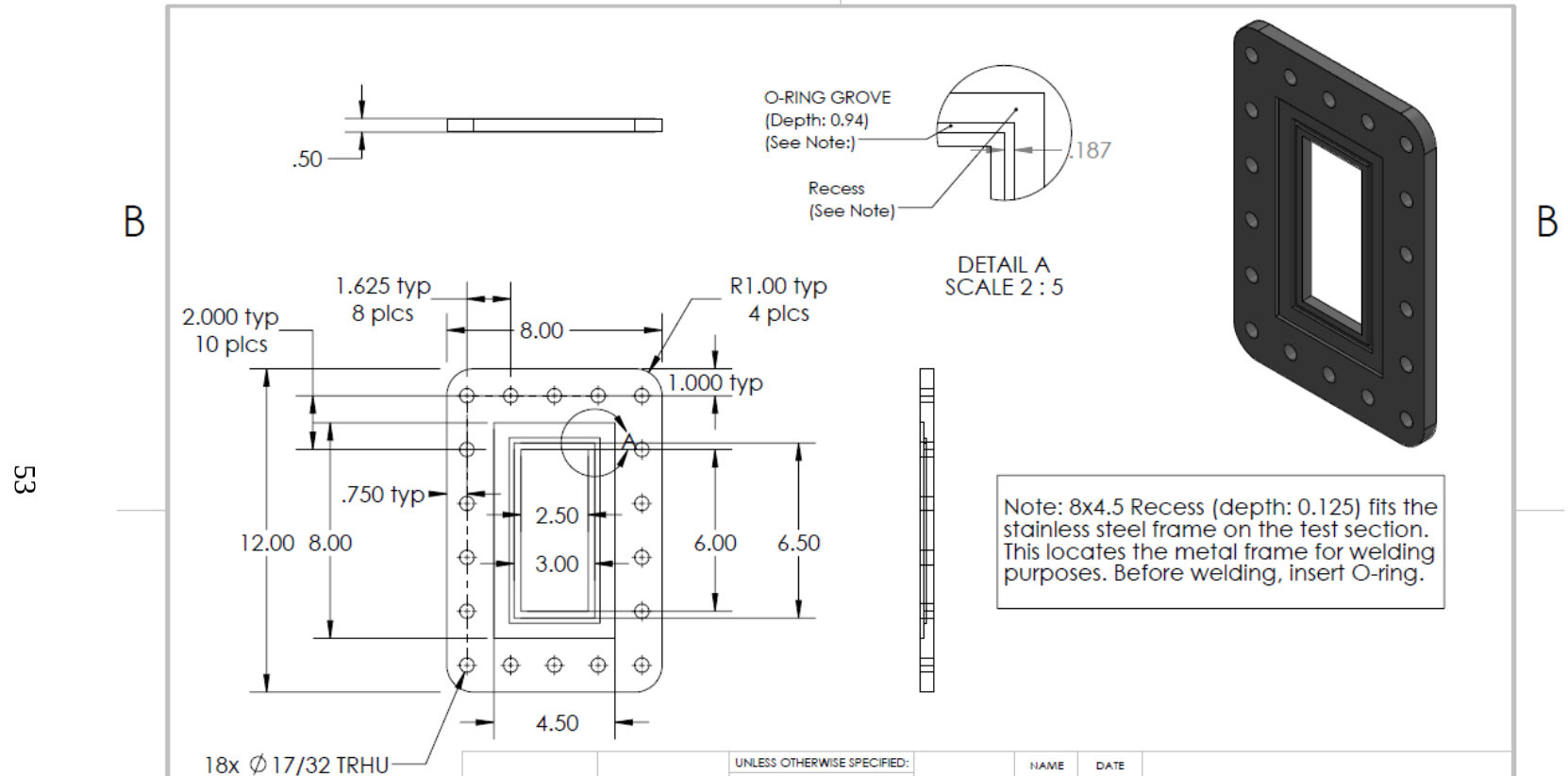
.50
O-RING GROVE
(Depth: 0.94)
(See Note:)
.187
Recess
(See Note)
DETAIL A
SCALE 2 : 5
1.625 typ
8 plcs
8.00
R1.00 typ
4 plcs
2.000 typ
10 plcs
1.000 typ
.750 typ
2.50
3.00
12.00
8.00
6.00
6.50
4.50
18x ∅17/32 TRHU
Note: 8x4.5 Recess (depth: 0.125) fits the stainless steel frame on the test section. This locates the metal frame for welding purposes. Before welding, insert O-ring.
UNLESS OTHERWISE SPECIFIED:
DIMENSIONS ARE IN INCHES
TOLERANCES:
ONE PLACE DECIMAL ± 0.08
TWO PLACE DECIMAL ± 0.04
THREE PLACE DECIMAL ± 0.005
INTERPRET GEOMETRIC TOLERANCING PER:
MATERIAL
STAINLESS STEEL
FINISH
DULL MILL FINISH
DO NOT SCALE DRAWING
NEXT ASSY
USED ON
APPLICATION
NAME
DATE
DRAWN
CHECKED
ENG APPR.
MFG APPR.
Q.A.
COMMENTS:
TITLE:
SIZE
A
DWG. NO.
Flange
REV
SCALE: 1:5
WEIGHT:
SHEET 1 OF 1

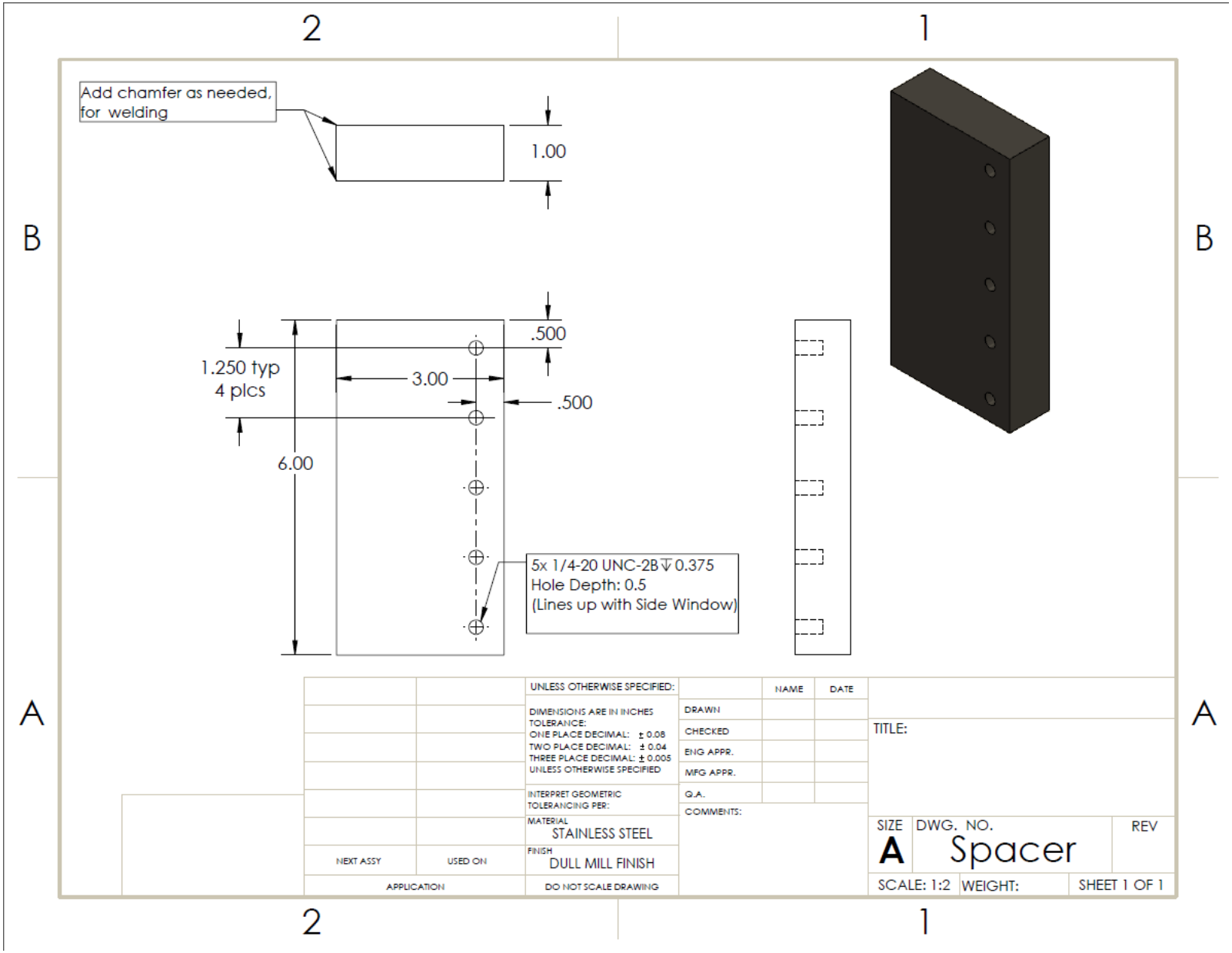
2
1
B
A
Add chamfer as needed,
for welding
1.00
.500
1.250 typ
4 plcs
3.00
.500
6.00
5x 1/4-20 UNC-2B ↧ 0.375
Hole Depth: 0.5
(Lines up with Side Window)
UNLESS OTHERWISE SPECIFIED:
DIMENSIONS ARE IN INCHES
TOLERANCE:
ONE PLACE DECIMAL: ± 0.08
TWO PLACE DECIMAL: ± 0.04
THREE PLACE DECIMAL: ± 0.005
UNLESS OTHERWISE SPECIFIED
INTERPRET GEOMETRIC TOLERANCING PER:
MATERIAL
STAINLESS STEEL
FINISH
DULL MILL FINISH
DO NOT SCALE DRAWING
NEXT ASSY
USED ON
APPLICATION
NAME
DATE
DRAWN
CHECKED
ENG APPR.
MFG APPR.
Q.A.
COMMENTS:
TITLE:
SIZE
A
DWG. NO.
Spacer
REV
SCALE: 1:2
WEIGHT:
SHEET 1 OF 1

5th Order Polynomial Contraction Drawing

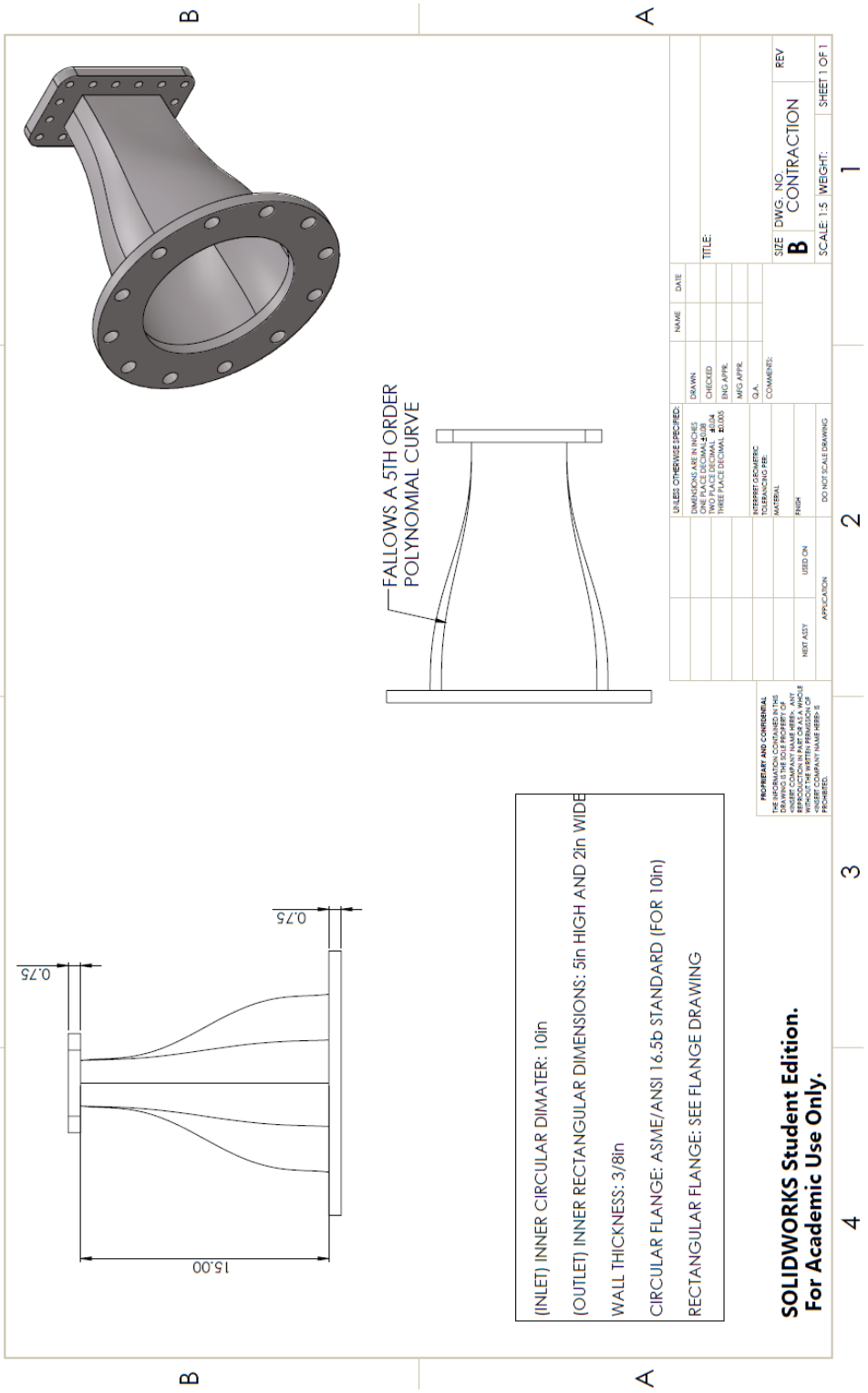

Expansion Drawings

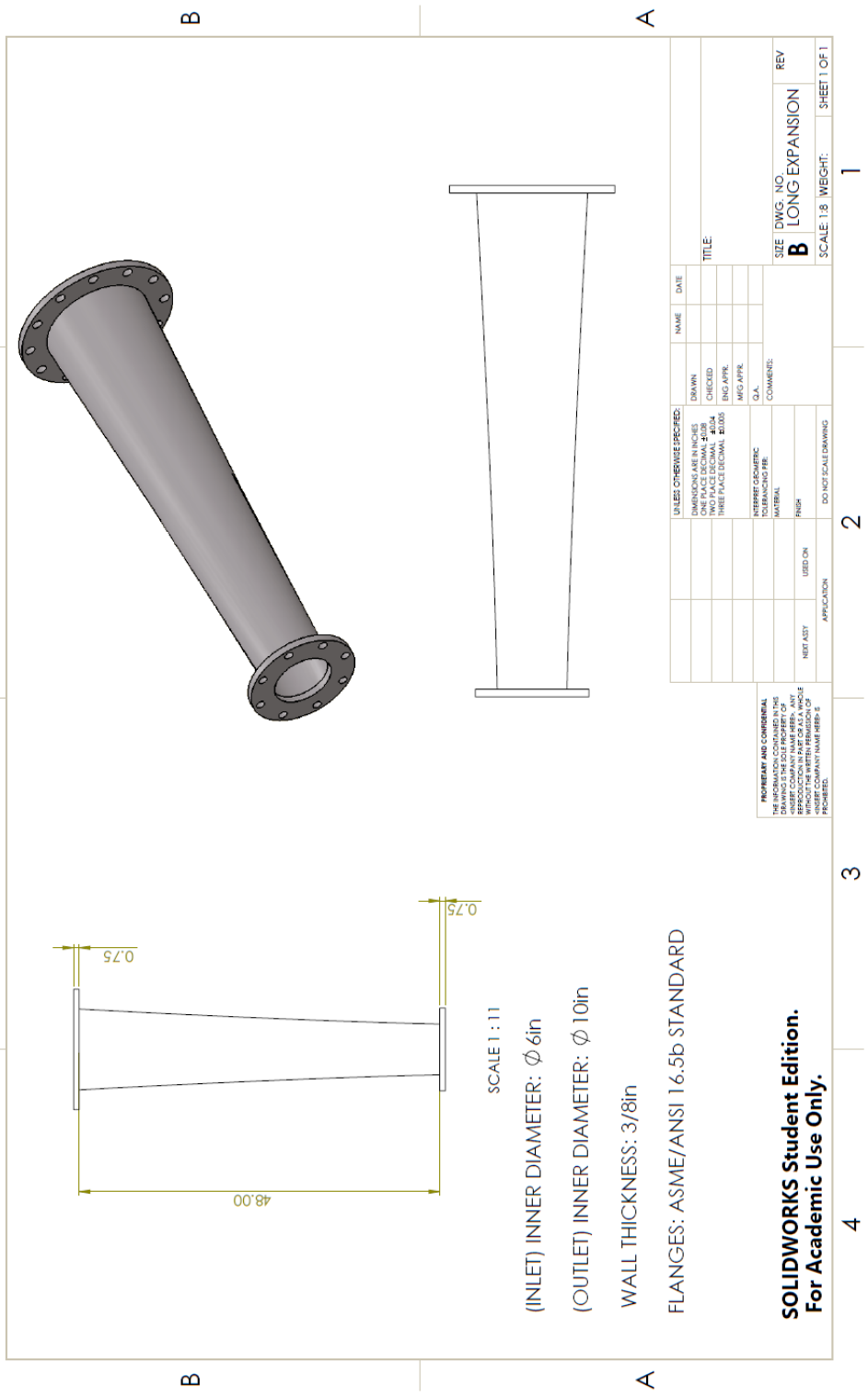

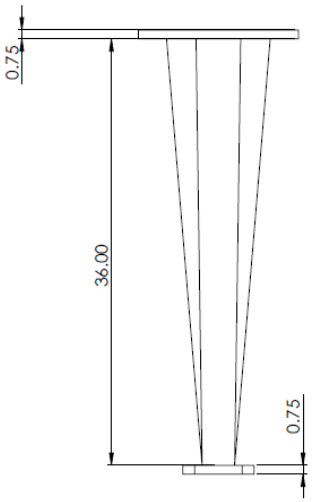

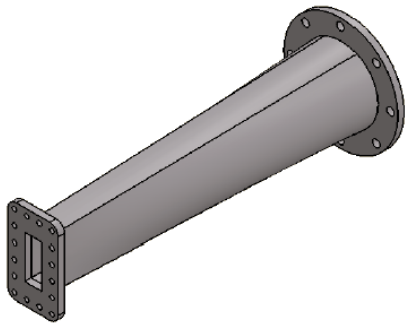

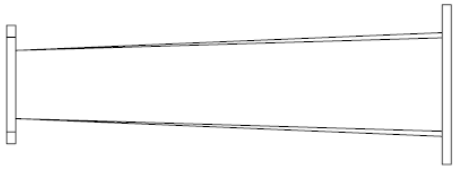

RECTANGULAR TO CIRCULAR EXPANSION:

(INLET) INNER RECTANGLE DIMENSIONS: 5in HIGH AND 2in WIDE

(OUTLET) INNER CIRCLE DIAMETER: 8in

WALL THICKNESS: 3/8in

CIRCULAR FLANGE: ASME/ANSI 16.5b STANDARD

RECTANGULAR FLANGE: SEE FLANGE DRAWING

SOLIDWORKS Student Edition.
For Academic Use Only.

		UNLESS OTHERWISE SPECIFIED:		NAME	DATE
		DIMENSIONS ARE IN INCHES ONE PLACE DECIMAL ±0.08 TWO PLACE DECIMAL ±0.04 THREE PLACE DECIMAL ±0.005	DRAWN		
			CHECKED		
			ENG APPR.		
			MFG APPR.		
		INTERPRET GEOMETRIC TOLERANCING PER:	Q.A.		
		MATERIAL	COMMENTS:		
NEXT ASSY	USED ON	FINISH			
APPLICATION		DO NOT SCALE DRAWING			

TITLE:

SIZE	DWG. NO.	REV
B	SHORT EXPANSION	

SCALE: 1:8 | WEIGHT: | SHEET 1 OF 1